Development Advance Online Articles. First posted online on 12 July 2016 as 10.1242/dev.135038
Access the most recent version at http://dev.biologists.org/lookup/doi/10.1242/dev.135038

An Ancestral Stomatal Patterning Module Revealed in the Non-Vascular Land Plant *Physcomitrella patens*

Robert Caine[1,$], Caspar C. Chater[2,4,$], Yasuko Kamisugi[3], Andrew C. Cuming[3], David J. Beerling[1,*], Julie E. Gray[2,*] and Andrew J. Fleming[1,*]

[1]Department of Animal and Plant Sciences, University of Sheffield, Sheffield S10 2TN, UK
[2]Department of Molecular Biology and Biotechnology, University of Sheffield, Sheffield S10 2TN, UK
[3]Centre for Plant Science, University of Leeds, Leeds LS2 9JT, UK
[4]Current address: Departamento de Biología Molecular de Plantas, Instituto de Biotecnología, Universidad Nacional Autónoma de Mexico Cuernavaca, Mexico

[$] Joint first authors
* Joint senior authors

Key words: Stomata, evolution, patterning, peptide signalling

Summary Statement

The genetic module controlling patterning of stomata in vascular plants also functions in non-vascular plants, consistent with the idea that it represents an ancestral mechanism in plant evolution.

ABSTRACT

The patterning of stomata plays a vital role in plant development and has emerged as a paradigm for the role of peptide signals in the spatial control of cellular differentiation. Research in Arabidopsis has identified a series of Epidermal Patterning Factors (EPFs) which interact with an array of membrane-localised receptors and associated proteins (encoded by *ERECTA* and *TMM* genes) to control stomatal density and distribution. However, although it is well established that stomata arose very early in the evolution of land plants, until now it has been unclear whether the established angiosperm stomatal patterning system represented by the EPF/TMM/ERECTA module reflects a conserved, universal mechanism in the plant kingdom. Here, we use molecular genetics to show that the moss *Physcomitrella patens* has conserved homologues of angiosperm *EPF*, *TMM* and at least one *ERECTA* gene which function together to permit the correct patterning of stomata and that, moreover, elements of the module retain function when transferred to Arabidopsis. Our data characterise the stomatal patterning system in an evolutionary distinct branch of plants and support the hypothesis that the EPF/TMM/ERECTA module represents an ancient patterning system.

INTRODUCTION

Stomata are microscopic pores present in the epidermis of all angiosperms and the majority of ferns and bryophytes whose evolution proved to be an essential step in the success and diversification of land plants over the past 400 million years (Beerling, 2007). In particular, this innovation, coupled with vascular tissues and a rooting system, enabled land plants to maintain hydration by regulating the plant-soil-atmosphere water flows under fluctuating environmental conditions (Berry et al., 2010; Raven, 2002; Vaten and Bergmann, 2012). Stomatal distribution is tightly regulated, both via endogenous developmental mechanisms which influence their number and pattern in different organs of the plant, and via modulation of these controls by a host of environmental factors (Chater et al., 2015; Geisler et al., 1998; Hunt and Gray, 2009; MacAlister et al., 2007). This spatial control of stomatal distribution, combined with the ease of scoring phenotype on the exposed epidermis, makes them an attractive system to investigate the control of patterning in plants, a major topic highlighted in the seminal work by Steeves and Sussex (1989).

Extensive molecular genetic analyses in the model flowering plant Arabidopsis have provided significant insight into the mechanisms controlling stomatal patterning and differentiation in angiosperms (Chater et al., 2015; Engineer et al., 2014; Pillitteri and Torii, 2012; Simmons and Bergmann, 2016). In Arabidopsis, negatively and positively acting secreted peptide signals (Epidermal Patterning Factors, EPFs and Epidermal Patterning Factor-like proteins, EPFLs) function to control where and when stomata form and ensure that stomata are separated from each other by at least one intervening epidermal cell, thus optimising leaf gas exchange (Abrash and Bergmann, 2010; Hara et al., 2007; Hara et al., 2009; Hunt et al., 2010; Hunt and Gray, 2009; Sugano et al., 2010). This ‘one cell spacing rule’ results from the stereotypical local pattern of cell divisions by which stomata form, accompanied by cross-talk between cells. The molecular mechanism enforcing the spacing rule involves EPF/Ls interacting with transmembrane receptors, including members of the *ERECTA* gene family (*ERECTA, ER*; *ERECTA-LIKE1*, *ERL1*, and *ERECTA-LIKE2*, *ERL2*) whose activity is modulated in stomatal precursor cells by the receptor-like protein TOO MANY MOUTHS (TMM) (Lee et al., 2015; Lee et al., 2012; Shpak et al., 2005; Torii, 2012). Binding of EPF/Ls entrains a well-characterised signal transduction pathway involving a series of mitogen activated protein kinases which leads to the cellular events of stomatal differentiation (Torii, 2015).

Little is known of the developmental mechanisms regulating stomatal patterning in early land plants. Fossil cuticles of 400-million year old small branching leafless vascular land plants such as *Cooksonia* indicate stomata were generally scattered more or less evenly across stem surfaces without clustering (Edwards et al., 1998) and these authors report that in the

Rhynie Chert fossil plants stomata commonly occur on 'an expanded portion of the axis just below the sporangium'. These observations suggest the existence of a stomatal patterning module early in land plant evolution but we have very limited information on the nature of the genetic module controlling this process. However, homologues of key genes regulating vascular land plant stomatal differentiation are present in the genome and are expressed during sporophyte development in the moss *Physcomitrella patens* (Chater et al., 2013; O'Donoghue et al., 2013; Ortiz-Ramírez et al., 2015; Vaten and Bergmann, 2012), a basal non-vascular land plant lineage with stomata. This suggests that genetic components involved in regulating stomatal spacing have been conserved between mosses and vascular plants. This notion is further supported by complementation work performed in Arabidopsis showing that *Physcomitrella patens* group 1A bHLH transcription factors can at least partially fulfil the function of their angiosperm counterparts in the regulation of stomatal development (MacAlister and Bergmann, 2011).

Here, we use molecular genetics to compare stomatal patterning systems in a bryophyte (*Physcomitrella patens*) and an angiosperm (*Arabidopsis thaliana*). We show that *P. patens* has an EPF/TMM/ERECTA module required for stomatal patterning fundamentally similar to that found in angiosperms and that elements of the module retain function when transferred to Arabidopsis. Our data characterise the stomatal patterning system in moss and are consistent with the hypothesis that the EPF/TMM/ERECTA module represents an ancient patterning system in plants.

RESULTS

To identify potential orthologues of angiosperm genes implemented in stomatal patterning in *P. patens*, we performed a bioinformatic analysis. As shown in **Fig. 1A** and **Fig. S1A**, a single homologue of Arabidopsis *EPF1* and *EPF2* exists in *P. patens*, *PpEPF1* (see also (Takata et al., 2013)). Similarly, the stomatal patterning protein TMM (which is encoded by a single gene in Arabidopsis) is homologous to a single gene in *P. patens*, termed *PpTMM* (Peterson et al., 2010) (**Fig. 1C** and **Fig. S1B**). The situation with the *ERECTA* genes is more complicated as six potential orthologues are found in the genome of *P. patens* (Villagarcia et al., 2012) (**Fig. 1E** and **Fig. S1C**).

To identify genes potentially involved in stomatal patterning we first interrogated a microarray database (O'Donoghue et al., 2013) to ascertain which *PpERECTA* gene/s showed upregulation of expression in the developing sporophyte. All the *PpERECTA* genes were expressed to some level in the sporophyte but only *PpERECTA1* was upregulated relative to protonemal tissue (**Fig. S2A**), and qRT-PCR analysis confirmed that *PpERECTA1* expression was significantly upregulated in the sporophyte (**Fig. S2B**). This was further indicated by the analysis of two other transcriptomic data sets accessible via phytozome V11

and the eFP browser at bar.utoronto.ca which showed a relatively high level of *PpERECTA1* expression in the sporophyte (**Fig. S2C,D**) (Goodstein et al., 2012; Ortiz-Ramírez et al., 2015; Winter et al., 2007). Taken together, the data suggested that *PpERECTA1* expression was increased in the sporophyte and, thus, might be involved in stomatal patterning. As shown in **Fig. 1B**,**D**,**F**, analysis of eFP Browser data for *PpEPF1*, *PpTMM* and *PpERECTA1* indicated an accumulation of the relevant transcripts in young sporophyte tissue.

Having identified genes encoding homologues for each of the components of the core *EPF/TMM/ERECTA* module involved in angiosperm stomatal patterning, we undertook a functional analysis in *P. patens* by creating a series of gene knock-outs and analysing stomatal patterning in the sporophytes of the transgenic plants. Interruption of the targeted locus in transgenic plants was confirmed via genomic PCR (**Fig. S3**). As shown in **Fig. 2A-F**, loss of *PpEPF1* function led to an increase in the number of stomata per capsule. The extra stomata formed at the appropriate location at the base of the sporophyte (**Fig. 2A,B**), *i.e.*, they did not extend ectopically into the flanks of the spore capsule. As a consequence, stomata in *ppepf1* knock-out mutant capsules frequently occurred in clusters that were not apparent in WT sporophytes, where most stomata are separated from each other by at least one neighbouring epidermal cell (**Fig. 2C,D**). Quantification confirmed an increased number of stomata per capsule in the sporophytes of three independently generated *ppepf1* knock-out lines (**Fig. 2E**). Expression analysis confirmed the absence (lines *ppepf1-2*, *ppepf1-3*) or greatly decreased transcript level (*ppepf1-1*) for *PpEPF1* in these plants (**Fig. 2F).** Interruption of the targeted locus in transgenic plants was verified via genomic PCR (**Fig. S3**)

We also characterised the outcome of increased expression of *PpEPF1* on stomatal formation by creating lines of transgenic *P. patens* in which the *PpEPF1* coding sequence was constitutively over-expressed via the rice actin promoter (**Fig. 2L**). Sporophytes of the transgenic plants displayed a phenotype with a greatly reduced number of stomata. At the base of the sporophyte stomata were sporadic (**Fig. 2G,H**) and the number of stomata per capsule significantly decreased in three independent lines over-expressing *PpEPF1* (**Fig. 2K**). Although the number of mature stomata was clearly decreased in the plants overexpressing *PpEPF1*, analysis of the epidermis at the base of the sporophytes of the transgenic plants indicated occasional division patterns suggestive of the formation of stomatal precursors which had failed to undergo further differentiation into the stomatal lineage (compare **Fig. 2I** and **2J**).

To investigate the role of the PpTMM receptor we generated independent knock-out lines. Examples of the range of phenotypes observed are shown in **Fig 3B-D** for comparison with the WT pattern (shown in **Fig. 3A**). Some capsules had exceptionally few stomata (**Fig. 3C**)

whereas others developed numerous stomata, many of which occurred in clusters (**Fig. 3D**). This variation was consistently observed across all 3 independent *pptmm* knock-out lines. Again, as with the *ppepf1* knock-out and WT lines, stomata formation remained restricted to the base of the capsule. Quantification of the transgenic sporophytes revealed that the number of stomata per capsule tended to be lower in the *pptmm* knock-out lines than in the WT control, although this was statistically significant only in the line *pptmm-3* (**Fig. 3E**). When the proportion of stomata forming in clusters (defined as stomata forming in pairs or higher order adjacent complexes) was measured, it was apparent that the *pptmm* knock-out lines had a higher number of stomata in clusters than WT (**Fig. 3F**). Interruption of the targeted locus in transgenic plants was verified via genomic PCR (**Fig. S3**) and expression analysis confirmed that the three *pptmm* knock-out lines contained no detectable *PpTMM* transcript (**Fig. 3G**).

We further investigated the role of *PpTMM* by analysing transgenic *P. patens* in which the *PpTMM* sequence was constitutively overexpressed (**Fig. 3M**). For this part of the investigation we were only able to identify a single transgenic line but analysis suggested that an increased level of *PpTMM* transcripts had little effect on stomatal patterning. There was a slight increase in the number of stomata per capsule (**Fig. 3H,I**) but quantification indicated that this was not statistically significant (**Fig. 3L).** The extent of stomatal clustering was similar to that observed in WT sporophytes (**Fig. 3J,K**).

To ascertain whether *P. patens* requires *ERECTA* gene functioning during stomatal development we next targeted the *PpERECTA1* gene. Only a single *PpERECTA1* knock-out line was identified and, as shown in **Fig. 4AB**, stomata formed in the appropriate position at the base of the sporophyte with no obvious difference in stomatal differentiation (**Fig. 4C,D)** and no effect on stomatal number per capsule (**Fig. 4E**). Loss of *PpERECTA1* gene expression in this line was confirmed by RT-PCR (**Fig. 4F**), as was interruption of the targeted locus via genomic PCR (**Fig. S3**). Since analysis of the *pperecta1* knockout was unable to establish a conclusive role for this component in stomatal development, further experiments were carried out. To understand if the *PpTMM* and *PpEPF1* genes were acting in the same pathway as *PpERECTA1* during stomatal development a series of double knock-out mutants were produced. Analysis of *ppepf1-erecta1* double knockouts indicated a diminished *ppepf1* phenotype. Thus, although more stomata per capsule developed compared to WT the increase was less than in the *ppepf1* mutant (**Fig. 4G**). An even more dramatic effect was observed when *pptmm-epf1* double knock-outs were generated. In this situation the phenotype of increased stomata per capsule observed in the *ppepf1* knock-out was found to be entirely dependent on the presence of a functional *PpTMM* gene (**Fig. 4H**). Finally, a *pptmm-pperecta1* double knock-out displayed a greater decrease in stomata per

capsule than observed in the single *pptmm* and *pperecta1* mutants (**Fig 4I**). Analysis of epidermal regions of capsules from the different knock-out combinations (**Fig. 4J-O)** suggested that, in addition to the differences in stomata number, loss of some *EPF/TMM/ERECTA* gene combinations influenced the positioning/form of stomata and the general pattern of cell division in the epidermis. For example, although loss of *PpERECTA1* in a *ppepf1* background led to a decrease in stomatal number per capsule, there was often an apparent disruption to the epidermal cell patterning in the vicinity of the stomata that were formed (**Fig. 4J,M**). In the case of the *ppepf1-pptmm* double knock-outs (which restored stomata number per capsule to wild-type levels), there were also alterations to the epidermal cell division planes from the patterns observed in the *ppepf1* or *pptmm* capsules (**Fig. 4 J,K and N**). Furthermore, guard cells that formed at the boundaries appeared stretched, taking on a shape akin to neighbouring epidermal pavement cells. This elongated guard cell conformation was also seen in the *pptmm-pperecta1* line (**Fig. 4L,O**). Analysis of the various double knock-out combinations described above confirmed the absence of the relevant transcripts (**Fig. 4P-R**) and interruption of the targeted loci (**Fig. S3**).

In addition to suppression of stomata formation, some EPF-like peptides in angiosperms have evolved to competitively inhibit EPF action (Lee et al., 2015; Ohki et al., 2011). Most notably, *AtEPFL9 (STOMAGEN)* has been shown to enhance stomata formation in Arabidopsis and overexpression of *STOMAGEN* leads to increased stomatal number in Arabidopsis (Hunt et al., 2010; Sugano et al., 2010). As indicated in Fig. 1 and Fig S2A, bioinformatic analysis indicates that the *P. patens* genome encodes a peptide similar to EPF2 (which in Arabidopsis inhibits stomatal development), but has no apparent equivalent to EPFL9/STOMAGEN (which in Arabidopsis antagonises the activity of EPF2 and stimulates stomatal development). To investigate whether the stomatal patterning system in *P. patens* could be disrupted by overexpression of the evolutionary distinct anatagonistic peptide STOMAGEN (**Fig. S4A**), we overexpressed the Arabidopsis *STOMAGEN* gene in a WT *P. patens* background. Our results indicated that although the *STOMAGEN* transcripts accumulated to a high level (**Fig. S4G**), there was no apparent phenotype in terms of altered numbers of stomata per capsule (**Fig. S4B,C,D**) although occasionally abnormal epidermal cells and aberrant guard cells were observed at the base of the transgenic capsules (**Fig. S4E,F**).

Since our data suggested that *PpEPF1*, *PpTMM* and *PpERECTA1* all play a role in stomatal patterning in *P. patens*, we investigated whether they might represent conserved functions by introducing the *P. patens* genes into the appropriate Arabidopsis genetic background, i.e., could they complement the cognate angiosperm gene function in stomatal patterning? For this experiment we focused on the putative *EPF* and *TMM* orthologues since the respective

mutants in Arabidopsis have clear phenotypes with respect to stomatal density and patterning. Thus in leaves loss of *AtEPF1 or AtEPF2* results in increased stomatal density, with stomatal clustering being especially pronounced in *atepf1* (Hara et al., 2007). In *atepf2* increased density is the result of increased entry of cells to the stomatal lineage which causes not only more stomata but also more small epidermal stomatal precursor cells (Hara et al., 2009; Hunt and Gray, 2009). In Arabidopsis *tmm*, stomatal phenotype varies depending on the organ. For example, in leaves stomatal density and clustering is markedly increased, in *tmm* inflorescence stems no stomata are found, and in the flower pedicel a gradient of stomatal density is observed. Thus, at the base of *tmm* pedicels there are no stomata, in the middle region a few stomata form, and at the apical region of the pedicel stomatal density exceeds wild-type and clustering is common (Bhave et al., 2009; Geisler et al., 1998; Yang and Sack, 1995).

When *PpEPF1* was constitutively overexpressed in *atepf1* we found that the mutant phenotype was partially rescued, with leaves having stomatal densities that were lower than in the *atepf1* background and which approached wild-type values (**Fig. 5A)**. When *PpEPF1* was overexpressed in the *atepf2* mutant background only a slight recovery of stomatal density occurred (**Fig. 5A**) and epidermal cell density was essentially unchanged to that observed in *atepf2* (**Fig. S5**). With respect to *PpTMM*, when this sequence was expressed in the Arabidopsis *attmm* mutant under control of an endogenous *AtTMM* promoter there was no overt restoration of stomatal density to wild-type values in leaves and stomatal clustering was still observed (**Fig. 5B**). However, when the pedicel was examined there was a partial rescue of the *attmm* phenotype. This was most obvious in the middle region where stomatal density was restored towards wild-type values whereas in the basal and apical regions stomatal densities were similar to those observed in the *tmm* mutant (**Fig 5C**).

DISCUSSION

The control of patterning is core to development and the *EPF/TMM/ERECTA* module has emerged has a paradigm for peptide signalling in plants to control the distribution of essential cellular complexes on the epidermis, the stomata. Although it is well established that stomata arose very early in the evolution of land plants, until now it has been unclear whether the angiosperm stomatal patterning system represents an ancient, universal mechanism in the plant kingdom. Our data indicate that an essentially similar system functions in the moss *P. patens*, providing strong evidence that the *EPF/TMM/ERECTA* module represents an ancestral patterning system for stomata. Mosses and flowering plants last shared a common ancestor over 400 million years ago (Ruszala et al., 2011) (Ruszala et al., 2011), suggesting that the leafless sporophytes of early vascular land plants may have

deployed a patterning module comprising of genes closely related to the *EPF/TMM/ERECTA* suite identified here.

Our data establish, firstly, that the genome of an extant bryophyte, *P. patens*, contains homologous sequences to all three components of the *EPF/TMM/ERECTA* module present in the angiosperm *A. thaliana* and that they are expressed at an appropriate time in development to play a role in stomatal patterning. Two of these components (*PpEPF1* and *PpTMM*) are present as single copy genes, consistent with them representing relatively ancient ancestral forms. The situation with the *ERECTA* gene family was more complicated, but our expression analysis, including the analysis of staged, dissected sporophyte tissue, allowed us to identify one member of the *ERECTA* family in *P. patens* (*PpERECTA1*) which was expressed at the appropriate time and place to play a role in stomata formation and which was therefore selected for further investigation (O'Donoghue et al., 2013).

Functional analysis of these three genes (*PpEPF1*, *PpTMM*, *PpERECTA1*) indicated that they are all involved in stomatal patterning in *P. patens* with roles not dissimilar to those played by their putative orthologues in Arabidopsis (Geisler et al., 1998; Hara et al., 2007; Hara et al., 2009; Hunt and Gray, 2009; Shpak et al., 2005; Yang and Sack, 1995). This was clearest with *PpEPF1*. Loss of this peptide led to an increase in stomatal clustering and in stomata per capsule whereas overexpression led to a decrease in stomata per capsule. This indicates a function directly comparable to that observed for *AtEPF1* and, to a lesser extent, *AtEPF2* in Arabidopsis where loss of function leads to an increase in leaf stomatal density and stomatal clustering (Hara et al., 2007; Hara et al., 2009; Hunt and Gray, 2009).

With respect to *PpTMM*, a more complicated picture emerged, consistent with the context-dependence of the *tmm* phenotype reported in Arabidopsis (Geisler et al., 1998; Yang and Sack, 1995). For example, in mature leaves of the *Arabidopsis attmm* mutant stomatal clustering is apparent and stomatal density is higher than wild-type, whereas at the base of the pedicels no stomata form, in the middle region some stomatal formation occurs (with some clustering), and at the top of the pedicel ectopic stomata form, leading to increased density and clustering relative to the wild-type (Bhave et al., 2009; Geisler et al., 1998). In the sporophyte of *P. patens* (where stomata only form at the base of the spore capsule) we observed an overall trend for a decrease in stomatal density and increase in clustering in the *pptmm* lines. However, these average values obscure significant spatial variation even within single spore capsules, so that on a given capsule it was not uncommon to observe both stomatal clustering and adjacent areas devoid of stomata, i.e., the phenotype encompassed elements observed on leaves and pedicels in Arabidopsis. The mechanistic basis of this variation awaits elucidation but the data indicate an overall conservation of sequence and function for TMM in *P. patens* and Arabidopsis and support an important ancestral role for

this protein in the modulation of stomatal patterning in leafless early land plants. It is possible that the regulation of stomatal stochasticity by TMM in early land plants enabled or facilitated the later evolution of distinct stomatal patterns in different parts of the plant. One possibility is that other peptides in *P. patens*, encoded by genes similar to Arabidopsis *EPFL6* (*CHALLAH*), *EPFL5*/*CHALLAH-LIKE1* and *EPFL4*/*CHALLAH-LIKE2*, play a role in inhibiting stomatal formation in the absence of *PpTMM*, as is the case in Arabidopsis (Abrash and Bergmann, 2010; Abrash et al., 2011). A recent bioinformatics study has identified 9 *PpEPFL*/*CHALLAH-like* genes which are upregulated in the developing sporophyte (Ortiz-Ramírez et al., 2015; Takata et al., 2013). These genes represent a target for future work to provide a deeper understanding of peptide signalling and stomatal patterning.

In Arabidopsis, TMM modulates the activity of ERECTA proteins and the action of AtEPF2 (and possibly AtEPF1) is dependent on TMM (Hara et al., 2007; Hunt and Gray, 2009; Lee et al., 2012). To test whether PpEPF1 action requires PpTMM we produced double mutant lines (*pptmm-epf1)* and found that the *ppepf1* phenotype was masked. Thus, there is an epistatic interaction between *PpTMM* and *PpEPF1* similar to the situation reported in Arabidopsis for EPF1 or EPF2 and TMM (Hara et al., 2007; Hara et al., 2009; Hunt and Gray, 2009).

Our analysis of *P. patens* sporophytes lacking *PpERECTA1* expression indicated no difference in stomatal number and only a discrete difference in the spacing of stomata. As only one knock-out line could be assessed we emphasise that this result should be interpreted with caution. However, analysis of *pperecta1* in combination with either *ppepf1* or *pptmm* indicated a more pronounced role for PpERECTA1 in stomatal patterning. For example, loss of *PpERECTA1* partially rescued the phenotype shown by the *ppepf1* knock-out mutant. The available data indicate that there are at least five other closely related *PpERECTA* genes expressed in the sporophyte (**Fig. 2C** and **Fig. S1C**) (Villagarcia et al., 2012), so the lack of phenotype in the single *PpERECTA1* knock-out mutant may reflect a degree of genetic redundancy in a manner similar to the redundant activity of this receptor family in Arabidopsis (Shpak et al., 2005). Further analysis of these *PpERECTA* genes in the context of *pptmm* and *ppepf1* mutants may improve our insight into the role of these genes in stomatal development.

Our experiments demonstrated that for both EPF1 and TMM conservation of function extends across the evolutionary distance separating bryophytes and angiosperms, with expression of *PpEPF1* and *PpTMM* coding sequences leading to a partial rescue of the mutant phenotype in the relevant Arabidopsis genetic backgrounds. Interestingly, overexpression of *PpEPF1* in the *atepf1* background was sufficient to restore stomatal number to near wild-type level whereas it was less able to rescue the related *atepf2* mutant

phenotype. *AtEPF1* has been implicated in the spacing patterning of stomata whereas *AtEPF2* is thought to be more important for the earlier asymmetric divisions required for angiosperm stomatal initiation (Hara et al., 2007; Hara et al., 2009; Hunt and Gray, 2009). Our data therefore support the idea of an ancient role for an EPF peptide ligand in stomatal patterning, with the evolution of the angiosperm *EPF* gene family being linked to acquisition of asymmetrically dividing cells in stomatal development (Hara et al., 2009; Hunt and Gray, 2009). In Arabidopsis the *EPF/L* gene family appears to have expanded over evolutionary time so that particular combinations of different ligands and receptors function in different organs. This divergence of EPF function linked to increased plant complexity is supported by the observed inability of the Arabidopsis STOMAGEN sequence to alter stomatal patterning in *P. patens*. The acquisition of such novel regulators of stomata formation may reflect an evolutionary trend to more complex developmental systems, enabling a flexible control of stomatal pattern to allow plants to adapt organs to specific environments (Abrash and Bergmann, 2010; Hronková et al., 2015; Hunt and Gray, 2009; Rychel et al., 2010; Shpak et al., 2005; Takata et al., 2013).

In conclusion, our results establish that the members of an EPF/TMM/ERECTA ligand-receptor system are conserved between bryophytes and angiosperms, both in terms of the presence and expression of the relevant genes and in the functional conservation of their role in stomatal patterning. Our data do not provide information on the conservation (or otherwise) of the molecular interactions between the components of the EPF/TMM/ERECTA module (which have only recently become well described in the more highly studied Arabidopsis system (Lee et al., 2015; Lee et al., 2012)) and this represents an area for future investigation. Finally, the acquisition of stomata is recognised as being of fundamental importance in the evolution of land plants (Beerling, 2007; Berry et al., 2010) and our data strongly support the proposition that the genetic system regulating stomatal patterning was recruited at an extremely early stage of land plant evolution, supporting the idea that extant stomata are of monophyletic origin (Beerling, 2007; Edwards et al., 1998).

MATERIALS AND METHODS

Plant materials and growth conditions

Physcomitrella patens subspecies patens (Hedwig) strain 'Gransden' protonemal tissue and gametophores were grown at 25°C continuous light (PAR 140 µmol m^{-2} s^{-1}) in a Sanyo MLR-350 cabinet for transformations and genotyping. For stomatal analyses, P. patens was grown on sterile peat pellets under sporulating conditions (Chater et al., 2011). *Arabidopsis thaliana* seeds were surface sterilised, stratified and grown on M3 Levington compost in Conviron growth cabinets at 10hr 22°C/ 14hr 16-18°C light/dark cycle; 70% relative humidity, PAR 120 µmol m^{-2} s^{-1}.

P. patens gene manipulation and expression analysis

The 5' and 3' flanking regions of targeted genes were amplified from *P. patens* genomic DNA and inserted into plasmids by conventional cloning using primers detailed in Sup Table 1. Resulting plasmids were used as PCR templates to amplify knock-out constructs. *PpEPF1* was blunt-end ligated into EcoRV digested pKS-Eco, then BsoBI digested, and a hygromycin selection cassette (obtained from pMBLH6bI) blunt-end ligated between 5' and 3' flanking regions to produce the *Ppepf* knock-out construct. The *pptmm* and p*perecta1* knock-out constructs were both created by blunt-end ligating 5' flanking sequences into Ecl136II digested pMBL5DLdelSN (a pMBL5 derivative) containing the NPTII cassette. Resulting plasmids were digested with EcoRV and 3' flanking sequences inserted via blunt-end ligation. To target the *PpEPF1* locus in the *pptmm-1* background the *Ppepf* knock-out construct was used. To target the *PpERECTA1* locus in the *pptmm-1* background, the NPTII cassette in *the pperecta* construct was replaced with an HPH cassette at KpnI and NsiI sites to produce a hygromycin-selective *pperecta* knock-out construct.

To target overexpression constructs of *PpEPF1*, *PpTMM* and *AtSTOMAGEN* to the neutral 108 locus, genes minus their ATG codon were amplified from P. patens cDNA (*PpEPF1*), genomic DNA (*PpTMM*) or Arabidopsis cDNA (*AtSTOMAGEN*). They were blunt-end ligated into NcoI digested pACT-nos1 which contains the rice Actin-1 promoter and adjoining 5' UTR (Horstmann et al., 2004; McElroy et al., 1990). pACT1-nos fused genes were PCR amplified, digested with KpnI, and ligated into Kpn1/SmaI digested pMBL5DL108 (Wallace et al., 2015).

Gene targeting and PEG-mediated transformation of P. patens was performed using PCR derived templates (Kamisugi et al., 2005; Schaefer et al., 1991). Confirmation of integration at target site was performed by genomic PCR analysis (Fig. S3). Briefly, for each independent line PCR was performed targeting a fragment spanning the 5' genomic

sequence to the transgene resistance cassette (Fig. S3B,D,F,H,J) or the 3' genomic sequence to the transgene resistance cassette (Fig. S3C,E, G, I, K). For each gene knock-out either two or three independent transgenic lines were generated and analysed, with the exception of *pperecta1* and *pptmm-erecta1* for which only one line was obtained showing correct gene targeting and no expressed transcript. Expression of transgenes and absence of expression of targeted knock-out genes was determined by RT-PCR using single stranded cDNA generated from extracted RNA by M-MLV Reverse Transcriptase (Fisher Scientific, UK). RNA was extracted using Spectrum™ Plant Total RNA Kit (Sigma, UK). For expression analysis in *ppepf1* and *pptmm* lines, 120 developing sporophytes per line were harvested and used to extract RNA. For other RT-PCR analysis gametophyte-sporophyte mix samples were collected for each line which contained 25 gametophores and approximately 15 developing sporophytes. For quantitative RT-PCR analysis of *PpERECTA1* transcript, relative expression was compared between RNA extracted from protonemal versus pooled sporophyte tissue (approx. 300 capsules per replicate: 100 immature, 100 mid-sized and 100 fully expanded- sporophytes) in triplicated experiments. RNA integrity was verified by electrophoresis and NanoDrop ND-8000 (Fisher Scientific, Loughborough, UK) and 1µg RNA used in reactions alongside three control 'housekeeping' transcripts (Le Bail et al., 2013; Wolf et al., 2010), according to (Luna et al., 2014) with slight modifications (Sup Data 1). Transcript abundance was assayed using Rotor-Gene SYBR Green PCR kit and a Corbett Rotor Gene 6000 (Qiagen, Venlo, Netherlands).

Arabidopsis thaliana gene manipulation

For complementation experiments *AtEPF2*pro and *AtEPF1*pro gene promoter sequences (Hunt and Gray, 2009) were amplified and ligated into KpnI digested pMDC99. Polished AscI digested *pMDC99::AtEPF1pro* was ligated with the *PpEPF1* gene product. AscI/PacI digested *pMDC99::AtEPF2pro* was ligated with the AscI-PpEPF1-PacI product to produce the *AtEPF2::PpEPF1* fusion. For overexpression of *PpEPF1* in Arabidopsis, cDNA was amplified and inserted into *pENTR/D-TOPO* downstream of the 35S promoter of *pCTAPi* (Rohila et al., 2004) using LR Clonase. *AtTMMpro::PpTMM* fusions were constructed by ligating the AscI-PpTMM-AscI PCR product with AscI digested *pENTR::AtTMMpro* to produce *pENTR::AtTMMpro::PpTMM*. The promoter gene construct was then transferred to the HGW destination vector (Karimi et al., 2002) using LR clonase (Invitrogen, UK). Arabidopsis wild-type and mutants *epf1-1*, *epf2-2*, and *tmm-1* in *Col-0* background (Hunt et al., 2010; Yang and Sack, 1995) were transformed using Agrobacterium-mediated floral dip (Clough and Bent, 1998). Transformants were selected and transgene insertion and expression verified by PCR and RT-PCR.

Plant phenotyping

Fully expanded (orange to brown coloured) spore capsules were fixed in modified Carnoy's solution (2:1 Ethanol: Glacial acetic acid) 6 to 7 weeks after fertilisation by flooding. Capsules of a similar size were dissected to remove associated spores, mounted between a bridge of cover slides in DH2O and stomata imaged with an Olympus BX-51 microscope fitted with an Olympus DP71 camera and Olympus U-RFL-T-200 UV lamp (Tokyo, Japan) equipped with an LP 400nm emission filter. Multiple fields of view were stacked and colour corrected using ImageJ. Min Intensity (bright-field) or Max Intensity (fluorescence) settings were used to compile flattened images.

Fully expanded Arabidopsis leaves were collected 7 to 8 weeks after germination, abaxial epidermal impressions produced and stomatal densities taken from 2 to 3 fields of view per leaf (Hunt et al., 2009). Pedicels were collected from 14 week old plants, fixed and cleared in modified Carnoy's, dissected longitudinally, rinsed in 0.5% diphenylboric acid-2-aminoethyl ester (DPBA) (Sigma-Aldrich, Gillingham, UK) and 0.1% Triton X-100 (v/v) for 30 seconds, then mounted as above. Images were collected using bright-field on an Olympus BX-51 microscope with accompanying 400nm fluorescence (pE-2 UV, CoolLED, Andover, UK) and 455nm emission filter to capture fluorescence and stacked using ImageJ. Stomata were counted in areas of 180.26 x 262.56µm approximately 300µm from where pedicels were excised at the base, halfway up the stem and 150µm. T2 and homozygous T3 plants were phenotyped. Statistical tests were performed using Graphpad Prism6 (GraphPad Software, La Jolla California, USA) and graphs were produced using SigmaPlot version 13 (Systat Software, San Jose, CA).

ACKNOWLEDGEMENTS

RC was supported by a NERC PhD studentship and the research further supported by funding from BBSRC (BB/J001805) to JEG and ERC (CDREG, 32998) to DJB. Thanks go to Dr Ana López Sánchez, Alexandra Casey, Rhys McDonough and Tim Fulton for laboratory assistance during the project.

AUTHOR CONTRIBUTIONS

RC, CCC, YK performed experiments; all authors contributed to the design of experiments and interpretation of data; JEG, DJB and AJF developed the concept and co-ordinated the research; AJF planned the original manuscript and all authors contributed to writing the final version.

REFERENCES

Abrash, E. B. and Bergmann, D. C. (2010). Regional specification of stomatal production by the putative ligand CHALLAH. *Development* **137**, 447-455.

Abrash, E. B., Davies, K. A. and Bergmann, D. C. (2011). Generation of Signaling Specificity in Arabidopsis by Spatially Restricted Buffering of Ligand-Receptor Interactions. *Plant Cell* **23**, 2864-2879.

Beerling, D. J. (2007). *The emerald planet : how plants changed Earth's history*. Oxford: Oxford University Press.

Berry, J. A., Beerling, D. J. and Franks, P. J. (2010). Stomata: key players in the earth system, past and present. *Current Opinion in Plant Biology* **13**, 233-240.

Bhave, N. S., Veley, K. M., Nadeau, J. A., Lucas, J. R., Bhave, S. L. and Sack, F. D. (2009). TOO MANY MOUTHS promotes cell fate progression in stomatal development of Arabidopsis stems. *Planta* **229**, 357-367.

Chater, C., Gray, J. E. and Beerling, D. J. (2013). Early evolutionary acquisition of stomatal control and development gene signalling networks. *Current Opinion in Plant Biology* **16**, 638-646.

Chater, C., Peng, K., Movahedi, M., Dunn, J. A., Walker, H. J., Liang, Y. K., McLachlan, D. H., Casson, S., Isner, J. C., Wilson, I., et al. (2015). Elevated CO2-Induced Responses in Stomata Require ABA and ABA Signaling. *Current Biology* **25**, 2709-2716.

Clough, S. J. and Bent, A. F. (1998). Floral dip: a simplified method for Agrobacterium-mediated transformation of Arabidopsis thaliana. *Plant Journal* **16**, 735-743.

Edwards, D., Kerp, H. and Hass, H. (1998). Stomata in early land plants: an anatomical and ecophysiological approach. *Journal of Experimental Botany* **49**, 255-278.

Engineer, C. B., Ghassemian, M., Anderson, J. C., Peck, S. C., Hu, H. H. and Schroeder, J. I. (2014). Carbonic anhydrases, EPF2 and a novel protease mediate CO2 control of stomatal development. *Nature* **513**, 246-+.

Felsenstein, J. (1985). Confidence Limits on Phylogenies: An Approach Using the Bootstrap. *Evolution* **39**, 783-791.

Geisler, M., Yang, M. and Sack, F. D. (1998). Divergent regulation of stomatal initiation and patterning in organ and suborgan regions of the Arabidopsis mutants too many mouths and four lips. *Planta* **205**, 522-530.

Goodstein, D. M., Shu, S., Howson, R., Neupane, R., Hayes, R. D., Fazo, J., Mitros, T., Dirks, W., Hellsten, U., Putnam, N., et al. (2012). Phytozome: a comparative platform for green plant genomics. *Nucleic Acids Res* **40**.

Hara, K., Kajita, R., Torii, K. U., Bergmann, D. C. and Kakimoto, T. (2007). The secretory peptide gene EPF1 enforces the stomatal one-cell-spacing rule. *Genes & Development* **21**, 1720-1725.

Hara, K., Yokoo, T., Kajita, R., Onishi, T., Yahata, S., Peterson, K. M., Torii, K. U. and Kakimoto, T. (2009). Epidermal Cell Density is Autoregulated via a Secretory Peptide, EPIDERMAL PATTERNING FACTOR 2 in Arabidopsis Leaves. *Plant and Cell Physiology* **50**, 1019-1031.

Horstmann, V., Huether, C. M., Jost, W., Reski, R. and Decker, E. L. (2004). Quantitative promoter analysis in Physcomitrella patens: a set of plant vectors activating gene expression within three orders of magnitude. *BMC Biotechnology* **4**, 13-13.

Hronková, M., Wiesnerová, D., Šimková, M., Skůpa, P., Dewitte, W., Vráblová, M., Zažímalová, E. and Šantrůček, J. (2015). Light-induced STOMAGEN-mediated stomatal development in Arabidopsis leaves. *Journal of Experimental Botany*.

Hunt, L., Bailey, K. J. and Gray, J. E. (2010). The signalling peptide EPFL9 is a positive regulator of stomatal development. *New Phytologist* **186**, 609-614.

Hunt, L. and Gray, J. E. (2009). The Signaling Peptide EPF2 Controls Asymmetric Cell Divisions during Stomatal Development. *Current Biology* **19**, 864-869.

Kamisugi, Y., Cuming, A. C. and Cove, D. J. (2005). Parameters determining the efficiency of gene targeting in the moss Physcomitrella patens. *Nucleic Acids Research* **33**, 10.

Karimi, M., Inze, D. and Depicker, A. (2002). GATEWAY vectors for Agrobacterium-mediated plant transformation. *Trends Plant Sci* **7**, 193-195.

Le Bail, A., Scholz, S. and Kost, B. (2013). Evaluation of Reference Genes for RT qPCR Analyses of Structure-Specific and Hormone Regulated Gene Expression in Physcomitrella patens Gametophytes. *Plos One* **8**.

Lee, J. S., Hnilova, M., Maes, M., Lin, Y. C. L., Putarjunan, A., Han, S. K., Avila, J. and Torii, K. U. (2015). Competitive binding of antagonistic peptides fine-tunes stomatal patterning. *Nature* **522**, 439-43.

Lee, J. S., Kuroha, T., Hnilova, M., Khatayevich, D., Kanaoka, M. M., McAbee, J. M., Sarikaya, M., Tamerler, C. and Torii, K. U. (2012). Direct interaction of ligand-receptor pairs specifying stomatal patterning. *Genes & Development* **26**, 126-136.

Luna, E., van Hulten, M., Zhang, Y. H., Berkowitz, O., Lopez, A., Petriacq, P., Sellwood, M. A., Chen, B. N., Burrell, M., van de Meene, A., et al. (2014). Plant perception of beta-aminobutyric acid is mediated by an aspartyl-tRNA synthetase. *Nature Chemical Biology* **10**, 450-456.

MacAlister, C. A. and Bergmann, D. C. (2011). Sequence and function of basic helix-loop-helix proteins required for stomatal development in Arabidopsis are deeply conserved in land plants. *Evolution & Development* **13**, 182-192.

MacAlister, C. A., Ohashi-Ito, K. and Bergmann, D. C. (2007). Transcription factor control of asymmetric cell divisions that establish the stomatal lineage. *Nature* **445**, 537-540.

McElroy, D., Zhang, W., Cao, J. and Wu, R. (1990). Isolation of an efficient actin promoter for use in rice transformation. *The Plant Cell* **2**, 163-171.

O'Donoghue, M. T., Chater, C., Wallace, S., Gray, J. E., Beerling, D. J. and Fleming, A. J. (2013). Genome-wide transcriptomic analysis of the sporophyte of the moss Physcomitrella patens. *Journal of Experimental Botany* **64**, 3567-3581.

Ohki, S., Takeuchi, M. and Mori, M. (2011). The NMR structure of stomagen reveals the basis of stomatal density regulation by plant peptide hormones. *Nature Communications* **2**, 512.

Ortiz-Ramírez, C., Hernandez-Coronado, M., Thamm, A., Catarino, B., Wang, M., Dolan, L., Feijó, J. A. and Becker, J. D. (2015). A transcriptome atlas of *Physcomitrella patens* provides insights into the evolution and development of land plants. *Molecular Plant*. **9**, 205-20

Peterson, K. M., Rychel, A. L. and Torii, K. U. (2010). Out of the Mouths of Plants: The Molecular Basis of the Evolution and Diversity of Stomatal Development. *Plant Cell* **22**, 296-306.

Pillitteri, L. J. and Torii, K. U. (2012). Mechanisms of Stomatal Development. In *Annual Review of Plant Biology, Vol 63* (ed. S. S. Merchant), pp. 591-614. Palo Alto: Annual Reviews.

Raven, J. A. (2002). Selection pressures on stomatal evolution. *New Phytologist* **153**, 371-386.

Rohila, J. S., Chen, M., Cerny, R. and Fromm, M. E. (2004). Improved tandem affinity purification tag and methods for isolation of protein heterocomplexes from plants. *Plant J* **38**, 172-181.

Ruszala, E. M., Beerling, D. J., Franks, P. J., Chater, C., Casson, S. A., Gray, J. E. and Hetherington, A. M. (2011). Land Plants Acquired Active Stomatal Control Early in Their Evolutionary History. *Current Biology* **21**, 1030-1035.

Rychel, A. L., Peterson, K. M. and Torii, K. U. (2010). Plant twitter: ligands under 140 amino acids enforcing stomatal patterning. *Journal of Plant Research* **123**, 275-280.

Saitou, N. and Nei, M. (1987). The neighbor-joining method: a new method for reconstructing phylogenetic trees. *Mol Biol Evol* **4**, 406-425.

Schaefer, D., Zryd, J. P., Knight, C. D. and Cove, D. J. (1991). Stable transformation of the moss Physcomitrella patens. *Mol Gen Genet* **226**, 418-424.

Shpak, E. D., McAbee, J. M., Pillitteri, L. J. and Torii, K. U. (2005). Stomatal patterning and differentiation by synergistic interactions of receptor kinases. *Science* **309**, 290-293.

Simmons, A. R. and Bergmann, D. C. (2016). Transcriptional control of cell fate in the stomatal lineage. *Current Opinion in Plant Biology* **29**, 1-8.

Sugano, S. S., Shimada, T., Imai, Y., Okawa, K., Tamai, A., Mori, M. and Hara-Nishimura, I. (2010). Stomagen positively regulates stomatal density in Arabidopsis. *Nature* **463**, 241-U130.

Takata, N., Yokota, K., Ohki, S., Mori, M., Taniguchi, T. and Kurita, M. (2013). Evolutionary Relationship and Structural Characterization of the EPF/EPFL Gene Family. *PLoS ONE* **8**, e65183.

Tamura, K., Stecher, G., Peterson, D., Filipski, A. and Kumar, S. (2013). MEGA6: Molecular Evolutionary Genetics Analysis version 6.0. *Mol Biol Evol* **30**, 2725-2729.

Torii, K. (2012). Mix-and-match: ligand–receptor pairs in stomatal development and beyond. *Trends Plant Sci.* **17**, 711-9.

Torii, K. U. (2015). Stomatal differentiation: the beginning and the end. *Curr Opin Plant Biol* **28**, 16-22.

Vaten, A. and Bergmann, D. C. (2012). Mechanisms of stomatal development: an evolutionary view. *Evodevo* **3**, 11.

Villagarcia, H., Morin, A.-C., Shpak, E. D. and Khodakovskaya, M. V. (2012). Modification of tomato growth by expression of truncated ERECTA protein from Arabidopsis thaliana. *Journal of Experimental Botany* **63**, 6493-6504.

Wallace, S., Chater, C. C., Kamisugi, Y., Cuming, A. C., Wellman, C. H., Beerling, D. J. and Fleming, A. J. (2015). Conservation of Male Sterility 2 function during spore and pollen wall development supports an evolutionarily early recruitment of a core component in the sporopollenin biosynthetic pathway. *New Phytologist* **205**, 390-401.

Winter, D., Vinegar, B., Nahal, H., Ammar, R., Wilson, G. V. and Provart, N. J. (2007). An "Electronic Fluorescent Pictograph" Browser for Exploring and Analyzing Large-Scale Biological Data Sets. *Plos One* **2**, 12.

Wolf, L., Rizzini, L., Stracke, R., Ulm, R. and Rensing, S. A. (2010). The Molecular and Physiological Responses of Physcomitrella patens to Ultraviolet-B Radiation. *Plant Physiology* **153**, 1123-1134.

Yang, M. and Sack, F. D. (1995). The too many mouths and four lips mutations affect stomatal production in arabidopsis. *Plant Cell* **7**, 2227-2239.

Figures

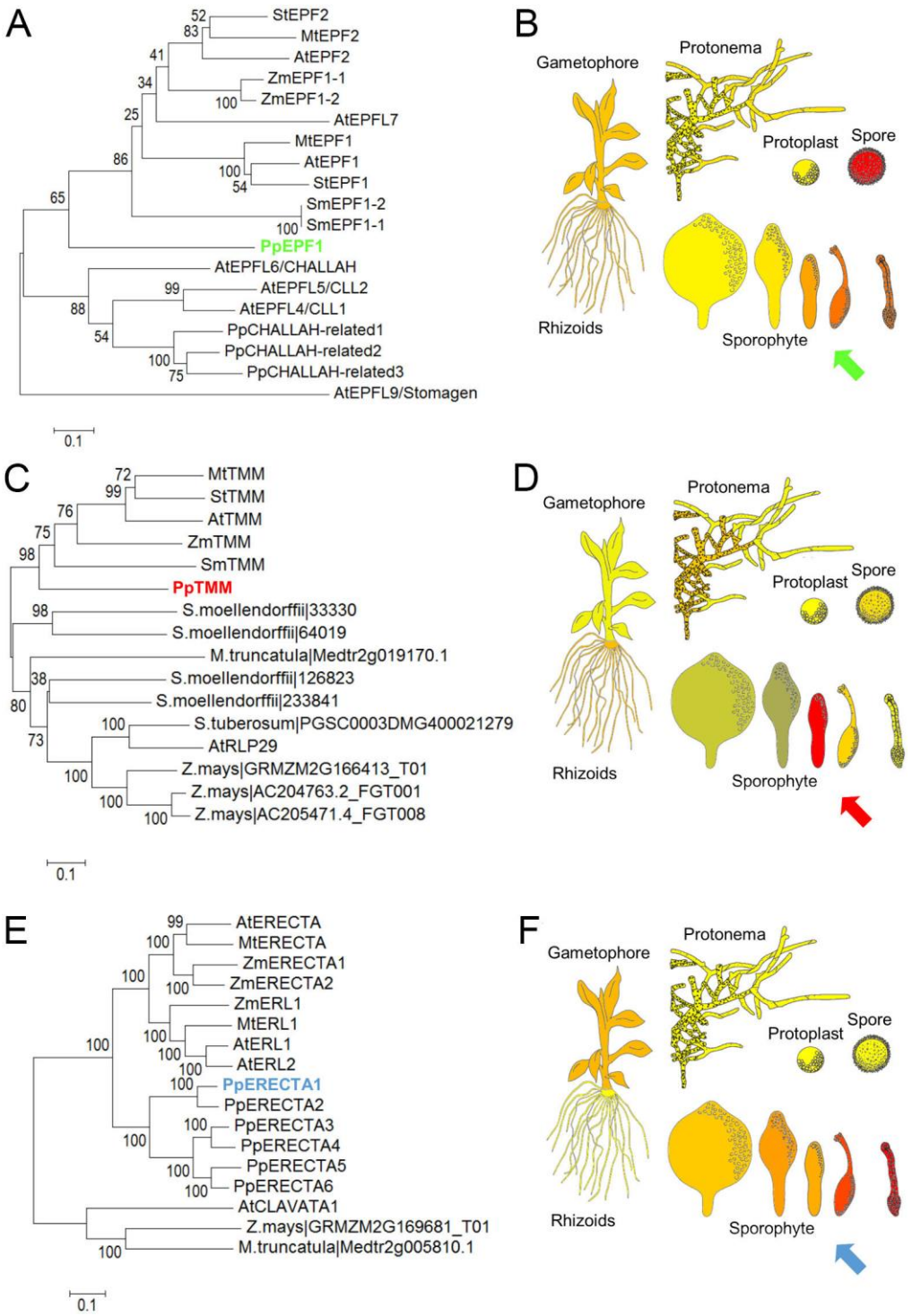

Figure 1. Phylogeny and expression profiles of stomatal patterning genes in *Physcomitrella patens* (**A,C,E**) Phylogenetic trees constructed using amino acid sequences of selected *Arabidopsis EPF1* (A), *TMM* (C) and *ERECTA* (E) gene family members based on Phytozome V11 (Goodstein et al., 2012), using the Neighbour-joining method (Saitou and

Nei, 1987; Takata et al., 2013) on MEGA6 (Tamura et al., 2013). The percentage of replicate trees in which the associated taxa clustered together in the bootstrap test (1000 replicates) are shown next to the branches (Felsenstein, 1985). Amino acid sequences from *P. patens* (Pp), *S. moellendorffii* (Sm), *Z. mays* (Zm), *S. tuberosum* (St), *M. truncatula* (Mt) and *A. thaliana* (At) were used to generate trees, except for *ERECTA*, where *S. moellendorffii* and *S. tuberosum* gene family members were omitted, owing to the large overall number of genes in the ERECTA family. For complete analyses of all three gene families see Fig. S1. (**B,D,F**) Expression profiles of (B) *PpEPF1* (D) *PpTMM* and (F) *PpERECTA1* based on microarray data taken from the *P. patens eFP browser* (Ortiz-Ramírez et al., 2015; Winter et al., 2007) for spore, protoplast, protonemal, gametophyte and sporophyte tissue. Red indicates a relatively high transcript level, with the arrows highlighting phases of sporophyte development when the respective genes appear to be relatively highly expressed. For the expression profiles of other *PpERECTA* gene family members see Fig. S2.

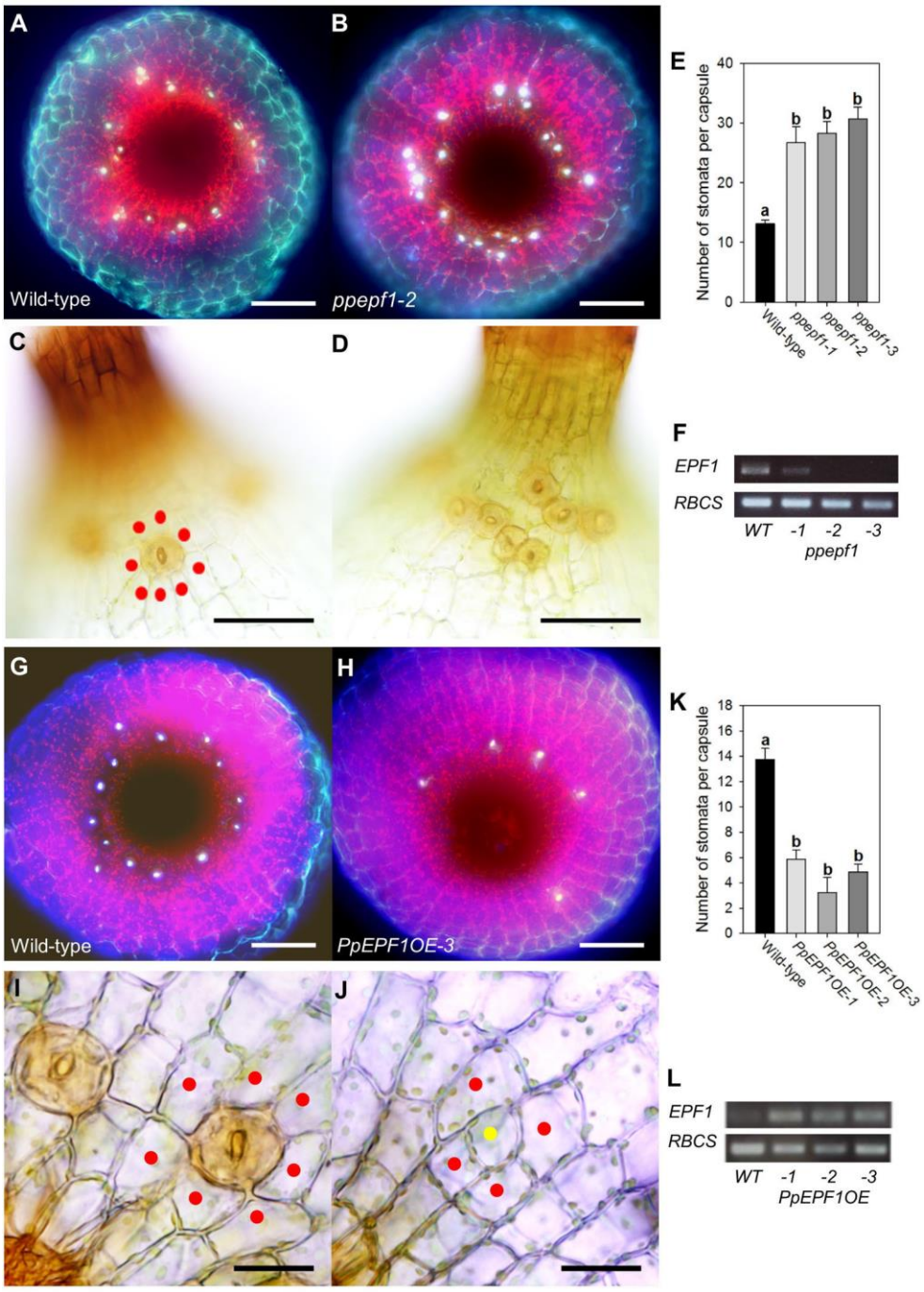

Figure 2. EPF function is conserved in *Physcomitrella patens*. (**A,B**) Fluorescence images of the base of the sporophyte from (A) WT (B) *ppepf1-2* plants. Stomata (bright white fluorescence) are spaced around the base in a ring with an increased number in *ppepf1-1*. (**C,D**) Bright-field lateral views of the sporophyte base from (C) WT (D) *ppepf1-2* plants. In WT, stomata are surrounded by epidermal cells (red dots) whereas in *ppepf1-2* stomata occur in clusters. (**E**) Number of stomata per capsule in wild-type and three *ppepf1* mutant lines. Lines indicated with different letters can be distinguished from each other ($P < 0.001$) (one-way ANOVA with multiple comparisons corrected using a Dunnett's test, n=7). (**F**) RT-

PCR analysis of the WT and transgenic lines shown in (E) with expression of (upper panel) *PpEPF* and (lower panel) a *PpRBCS* control. (**G,H**) Fluorescence images of the base of the sporophyte from (G) WT (H) *PpEPF1OE* plants. Fewer stomata are visible in the *PpEPF1OE* sporophyte. (**I,J)** Bright-field lateral views of the sporophyte base from (I) WT (J) *PpEPF1OE* plants with a possible stomatal precursor (yellow dot) indicated (**K**) Number of stomata per capsule in wild-type and three *PpEPFOE* mutant lines. Lines indicated with different letters can be distinguished from each other ($P < 0.001$) (one-way ANOVA with multiple comparisons corrected using a Dunnett's test, n=8). (**L**) RT-PCR analysis of the WT and transgenic lines shown in (K) with expression of (upper panel) *PpEPF1* and (lower panel) *PpRBCS* control transcript. Scale bars: A,B,G,H = 100μm; C,D = 50μm; I,J= 25 μm. Error bars = s.e.m.

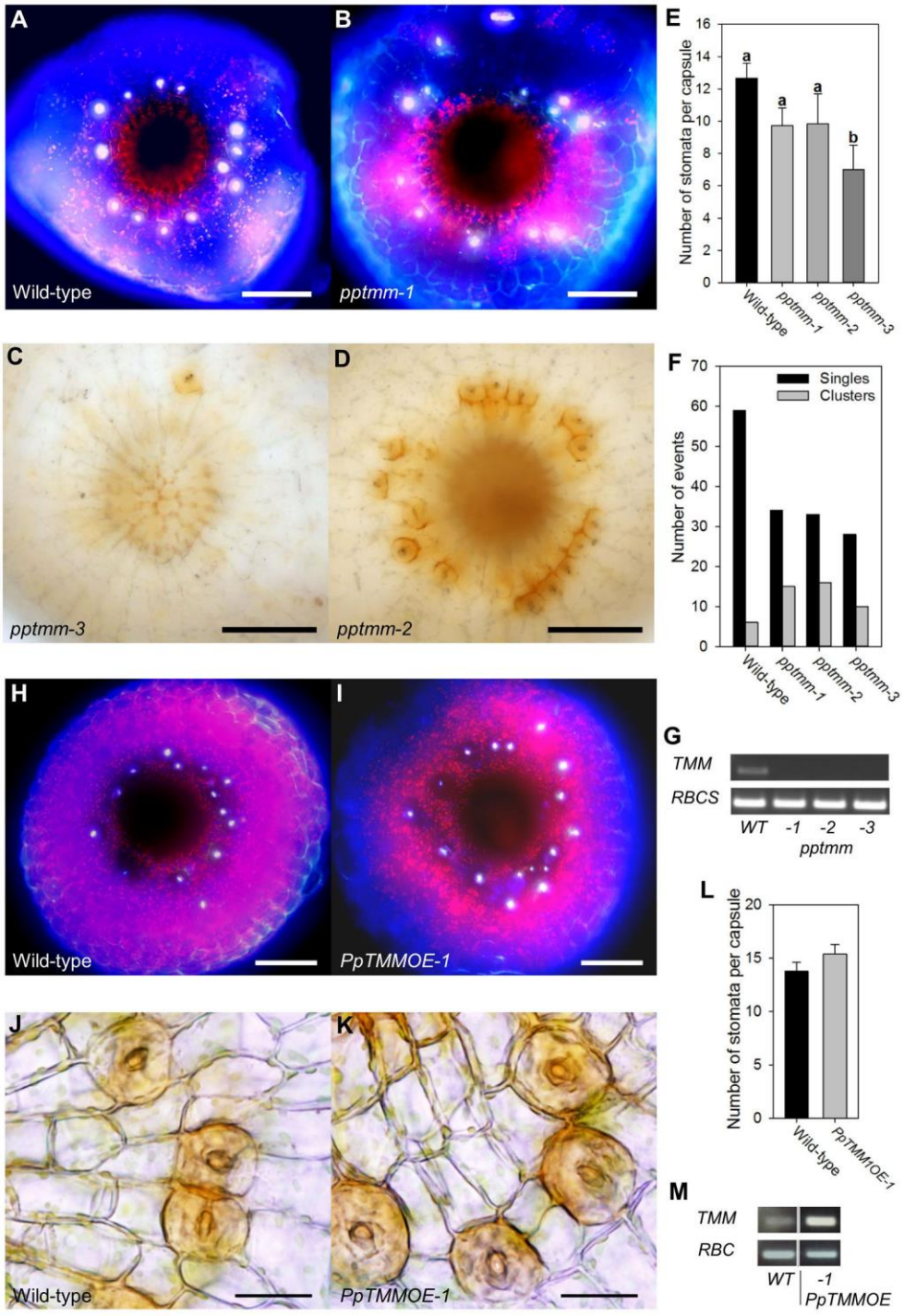

Figure 3. TMM functions in stomatal patterning in *Physcomitrella patens*. (**A,B**) Fluorescence images of the base of the sporophyte from (A) WT (B) *pptmm-1* plants. The pattern of stomata (bright white fluorescence) is disrupted in the *pptmm-1* mutant. (**C,D**) Bright-field lateral views of the sporophyte base from two transgenic lines: (C) *pptmm-3* (D) *pptmm-2*. The number and patterning of stomata varies from plant to plant in each of the three independent *pptmm* lines. (**E**) Number of stomata per capsule in wild-type and three

pptmm mutant lines. Lines indicated with different letters can be distinguished from each other ($P < 0.05$) (one-way ANOVA with multiple comparisons corrected using a Dunnett's test, $n>6$). (**F**) Percentage of stomata in clusters in the lines shown in (E). (**G**) RT-PCR analysis of the WT and transgenic lines shown in (E) with expression of (upper panel) *PpTMM* and (lower panel) *PpRBCS* control transcript. (**H,I**) Fluorescence images of the base of the sporophyte of (H) WT and (I) *PpTMMOE* plants. (**J,K**) Bright-field lateral views of the sporophyte base from (J) WT and (K) *PpTMMOE* plants (**L**) Number of stomata per capsule in wild-type and *PpTMMOE* line. No significant difference ($P< 0.05$) was found between the lines (one-way ANOVA with multiple comparisons corrected using a Dunnett's test, $n=8$). (**M**) RT-PCR analysis of the WT and transgenic line shown in (L) with expression of (upper panel) *PpTMM* and (lower panel) *PpRBCS* control transcript.

Scale bars: A,B,H,I = 100μm;C,D = 50μm; J,K= 25 μm. Error bars = s.e.m.

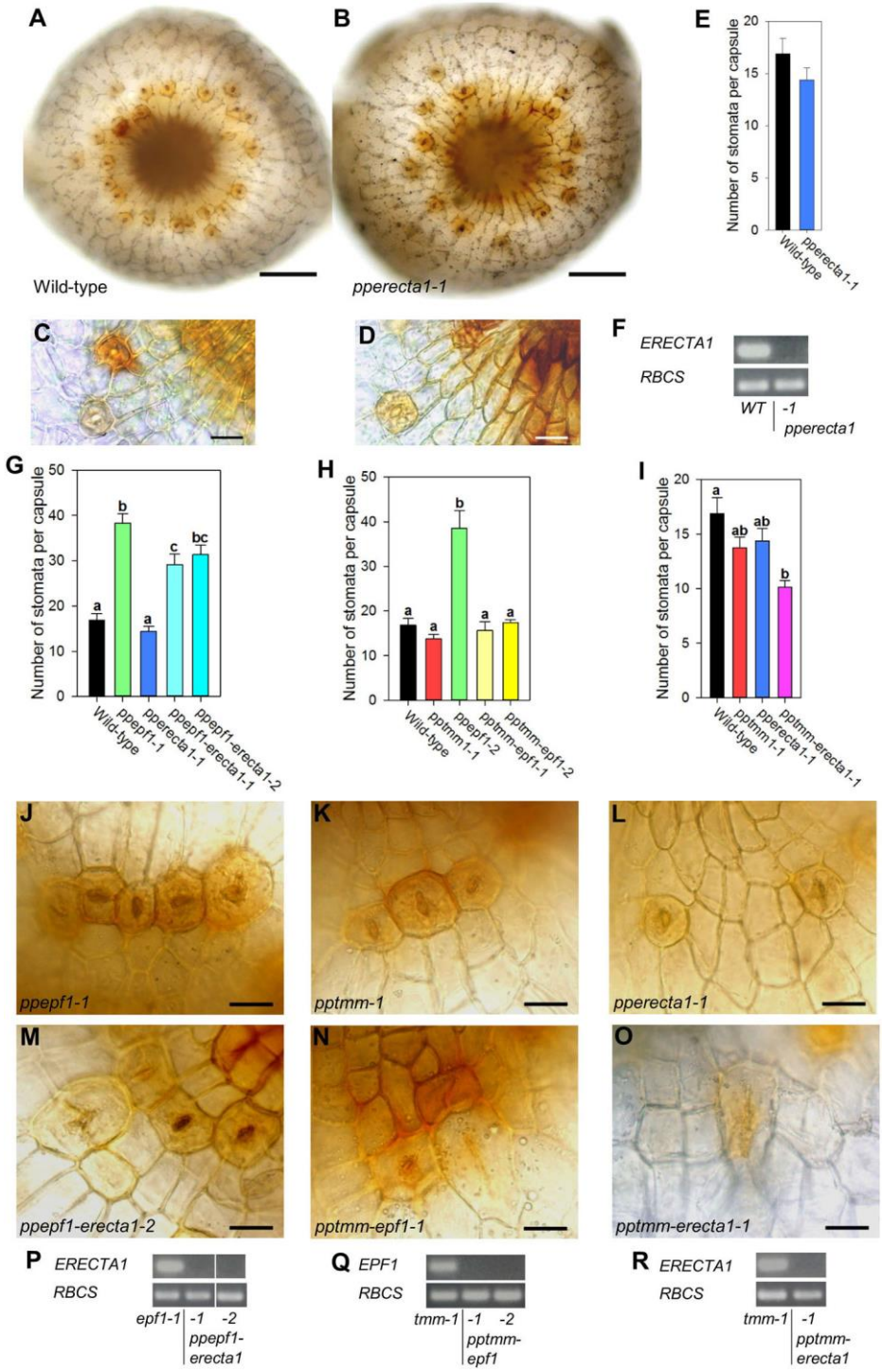

Figure 4. Epistasis between *PpEPF1*, *PpTMM* and *PpERECTA1* supports a concerted role in stomatal patterning (**A,B**) Bright field images of the base of the sporophyte from (A) WT and (B) *pperecta1-1* plants. (**C,D**) Bright-field lateral views of the sporophyte base from (C) WT and (D) *pperecta1-1* plants. (**E**) Number of stomata per capsule in wild-type and a *pperecta1-1* mutant line. No significant difference ($P < 0.05$) was found between the lines (one-way ANOVA with multiple comparisons corrected using a Dunnett's test, n=8). (**F**) RT-

PCR analysis of WT and *pperecta1-1* with expression of (upper panel) *PpERECTA1* and (lower panel) *PpRBCS* control transcript. (**G, H, I**) Number of stomata per capsule in: (G) *ppepf1-erecta1* (H) *pptmm-epf1* and (I) *pptmm-pperecta1* double mutants. Within each panel lines indicated with different letters can be distinguished from each other ($p<0.05$) (one-way ANOVA with multiple comparisons corrected using a Tukey test, n=8). (**J-O**) Bright-field lateral views of the base of sporophytes from (J) *ppepf1* (K) *pptmm* (L) *pperecta1* (M) *ppepf1-erecta1-2* (N) *pptmm-epf1-1* and (O) *pptmm-erecta1-1* lines. (**P-R**) RT-PCR analysis of the mutant lines shown M-O with the upper panel showing the transcript detection for (P,R) *PpERECTA1* (Q) *PpEPF1*, as indicated. Lower panel in each case indicates transcript detection for a *PpRBCS* control. Scale bars: A,B= 100μm; C,D, J-0 = 25 μm. Error bars G-I = s.e.m.

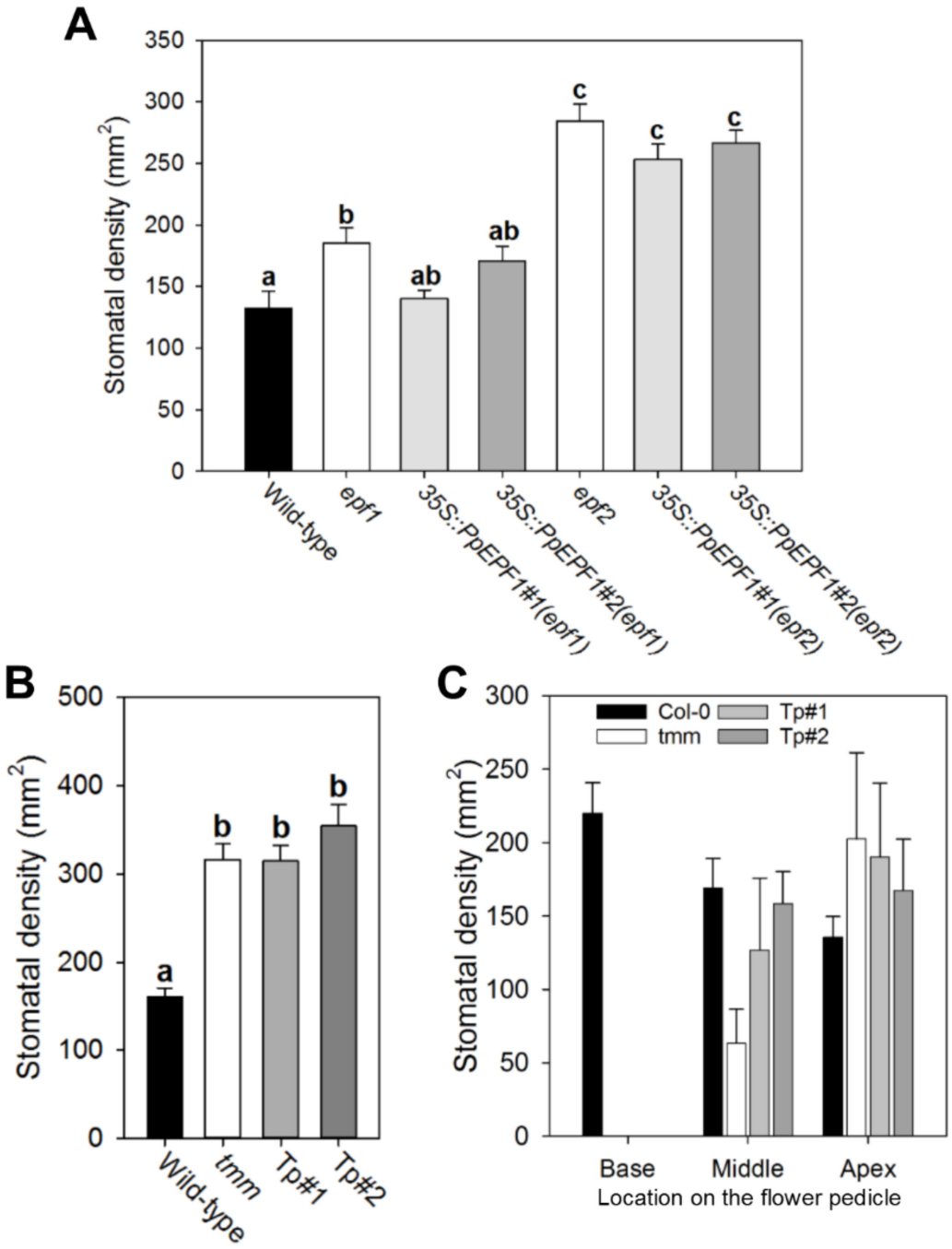

Figure 5. *PpEPF1* and *PpTMM* can partially rescue Arabidopsis stomatal density phenotypes. (**A**) Stomatal density in leaves in a series of lines of Arabidopsis thaliana either lacking *AtEPF1* (*epf1*) or *AtEPF2* (*epf2*) and overexpressing the *PpEPF1* sequence (35S::*PpEPF1*). Stomatal density in WT leaves is shown as a control. (**B**) As in (A) but for two lines of the Arabidopsis *tmm* mutant complemented with the *PpTMM* sequence under control of the native *AtTMM* promoter (Tp). In (A) and (B), Lines indicated with different letters can be distinguished from each other (one-way ANOVA with multiple comparisons corrected using a Tukey test, n=6 (**A**), n =8 (**B**), $P<0.05$). (**C**) As in (B) but for the phenotype observed in base, middle or apex of the flower pedicel (as indicated). Error bars = s.e.m.

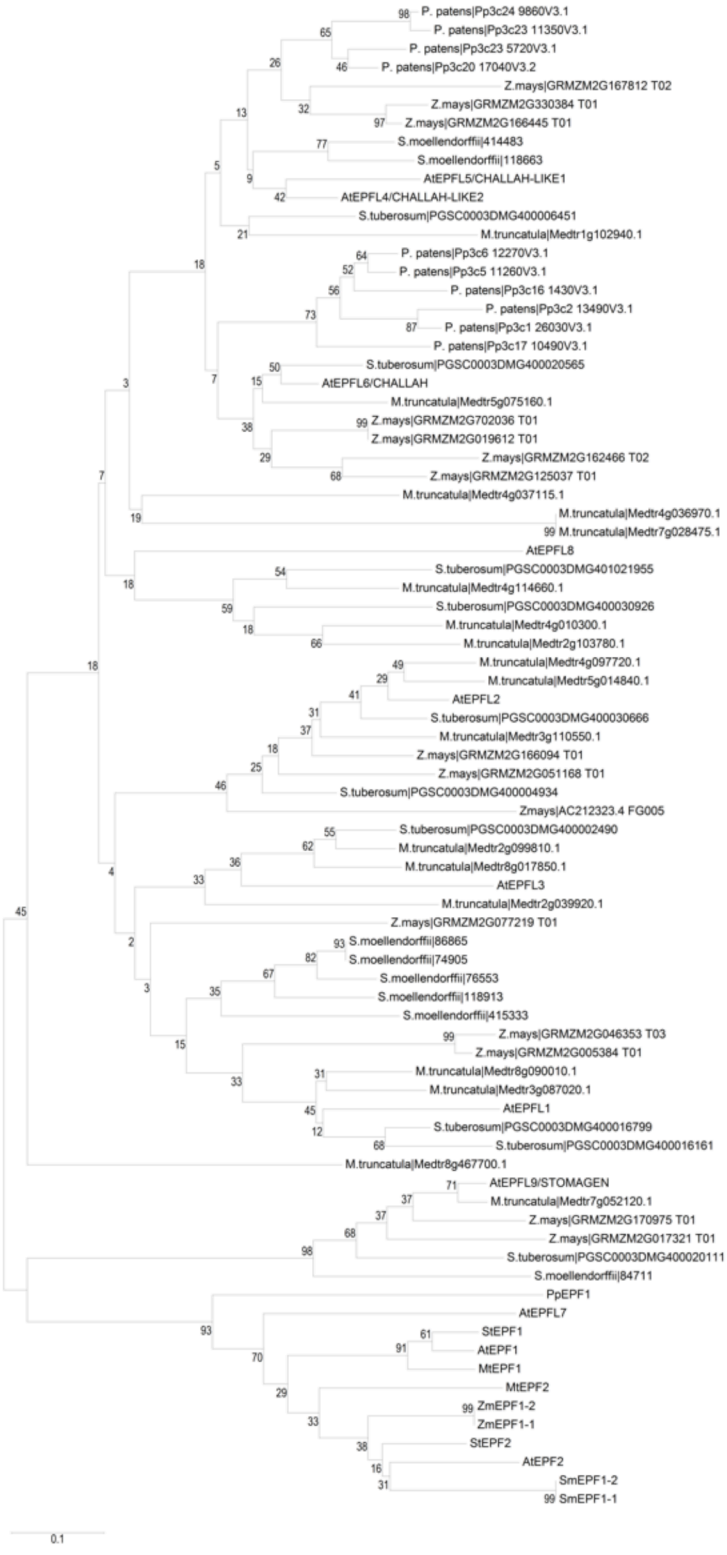

Fig S1A Phylogenetic tree for EPF

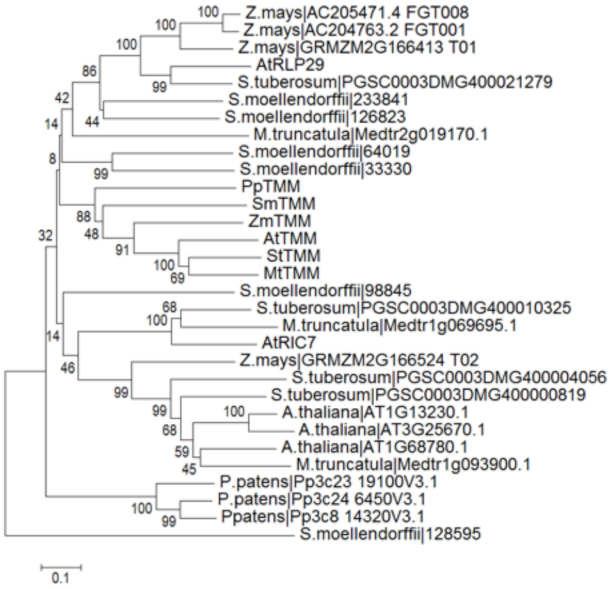

Fig S1B Phylogenetic tree for TMM

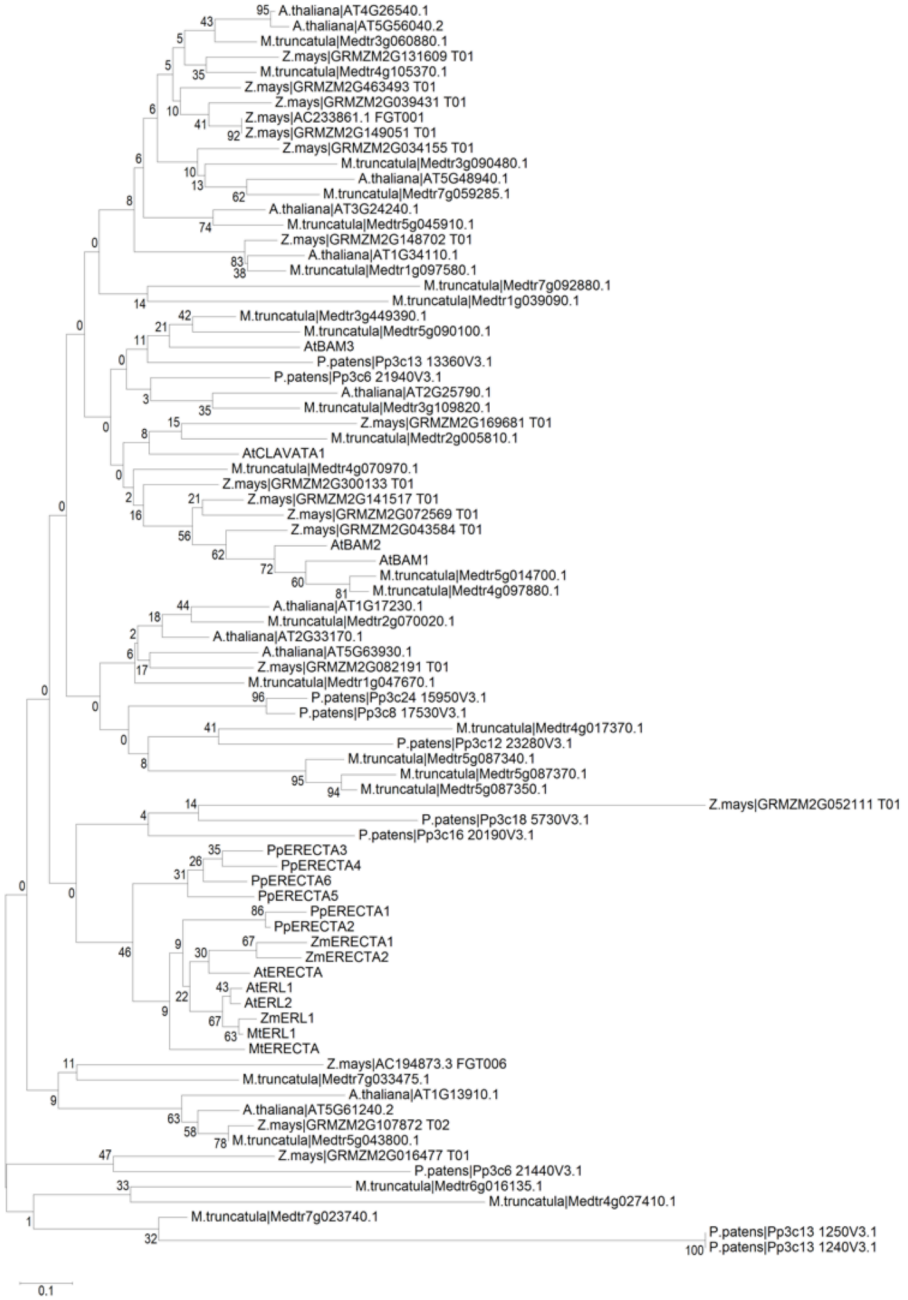

Fig S1C Phylogenetic tree for ERECTA

Fig. S1 Extended phylogenetic trees for *EPF*, *TMM* and *ERECTA* gene families
Evolutionary relationships of **(A)** *Epidermal Patterning Factor* (*EPF*) and *Epidermal Patterning Factor-like* (*EPFL*) genes; **(B)** *TOO MANY MOUTHS* (*TMM*) genes; and **(C)** *ERECTA* and *ERECTA-like* genes based on amino acid sequence alignments from selected land plant lineages**.** Gene family members related to *A. thaliana EPF1, TMM and ERECTA* from *P. patens, S. moellendorffii*, *Z. mays*, *S. tuberosum, M. truncatula* and *A. thaliana* (as indicated) were identified via phytozome gene family predictions and manual methods (Goodstein et al., 2012). For the *ERECTA* phylogeny *S. moellendorffii* and *S. tuberosum* have been emitted from the analysis due to the large number of gene representatives overall in this family. Sequences were aligned using the MUSCLE (Edgar, 2004) alignment tool on MEGA6 (Tamura et al., 2013).The evolutionary history was inferred using the Neighbor-Joining method (Saitou and Nei, 1987) on MEGA6 (Tamura et al., 2013). The optimal trees with the sum of branch length = 13.422 (EPF); 9.345 (TMM); 20.7487 (ERECTA) are shown. The percentage of replicate trees in which the associated taxa clustered together in the bootstrap test (1000 replicates) are shown next to the branches (Felsenstein, 1985). The tree is drawn to scale, with branch lengths in the same units as those of the evolutionary distances used to infer the phylogenetic tree. The evolutionary distances were computed using the Poisson correction method (Zuckerkandl and Pauling, 1965) and are in the units of the number of amino acid substitutions per site. For EPF/L represenatives the analysis involved 79 amino acid sequences. All positions containing gaps and missing data were eliminated. There were a total of 33 positions in the final dataset. For TMM the analysis involved 31 amino acid sequences. All positions containing gaps and missing data were eliminated. There were a total of 185 positions in the final dataset. Fore ERECTA the analysis involved 82 amino acid sequences. All positions containing gaps and missing data were eliminated. There were a total of 24 positions in the final dataset. See Table S1 for accession numbers not indicated in the trees.

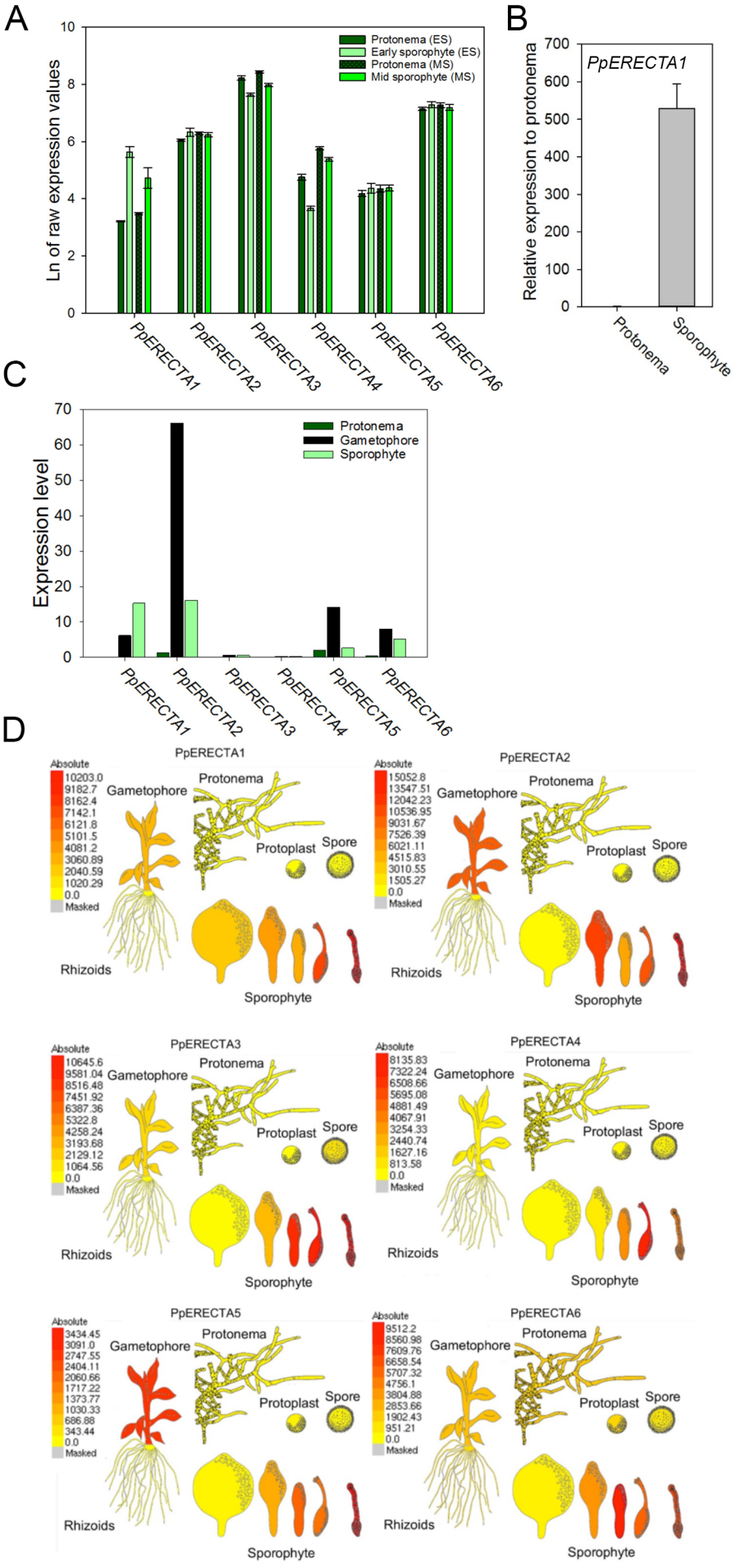

Fig. S2 Expression profiles of *PpERECTA* genes.

(A) Expression levels of 6 *PpERECTA* genes in early (ES) and mid-stage (MS) sporophytes derived from microarray data (O'Donaghue et al, 2013). The expression in each sporophyte stage can be compared with the transcript level in protonema taken from the equivalent colony stage.

(B) qPCR analysis of *PpERECTA1* expression in protonemal and sporophyte tissue.
Expression relative to an actin control gene has been set at 1 for the protonemal tissue, indicating a 500-fold relative increase in *PpERECTA1* expression in the sporophyte.

(C) Expression levels of 6 *PpERECTA* genes in protonema, gametophores and sporophytes. Data derived from the Phytozome gene atlas (vs 11) (Goodstein et al., 2012)

(D) Expression profiles of 6 *PpERECTA* genes derived from microarray data on the *P. patens eFP browser* (Ortiz-Ramirez et al., 2016) for spore, protoplast, protonemal, gametophyte and sporophyte tissue. Absolute expression values are provided to illustrate differential expression between related *PpERECTA* family members.

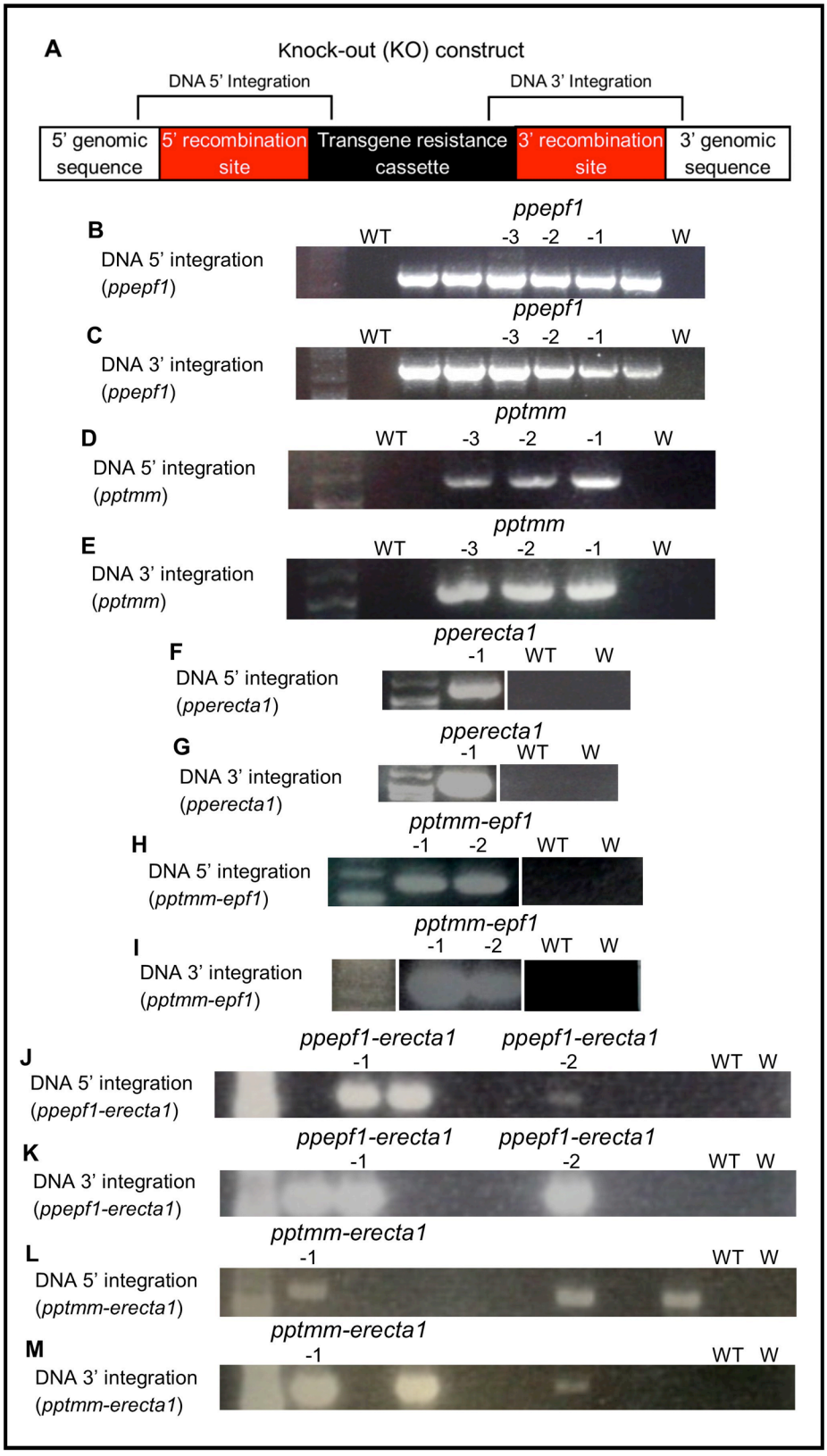

Fig. S3 Molecular analysis of gene knock-out lines

(A) Schematic of approach taken to confirm gene knock-outs. To verify 5' genomic integration, PCR was performed on mutant lines targeting a fragment spanning from the 5' genomic sequence to the transgene resistance cassette. To verify 3' genomic integration, PCR was performed to verify the presence of a fragment spanning from the transgene resistance cassette to the 3' genomic sequence. (B-M) Gel images of PCR products illustrating targeted integration of the KO construct at both the 5' and 3' regions of the genomic loci of mutants: *ppepf1* (B,C); *pptmm* (D,E); *pperecta1* (F,G); *pptmm-epf1* (H,I); *ppepf1-erecta1* (J,K); and *pptmm-erecta1* (L,M). Each lane with a number indicates an individual line taken forward and used for phenotypic analysis. Lanes showing a band but no number indicate potential KO lines obtained but not taken forward for phenotyping. WT refers to a Wild-type sample DNA and W refers to a water sample control. Ladders are included on the left of each gel shot but owing to variation in exposure are not always visible. Primers used are listed in Table S2.

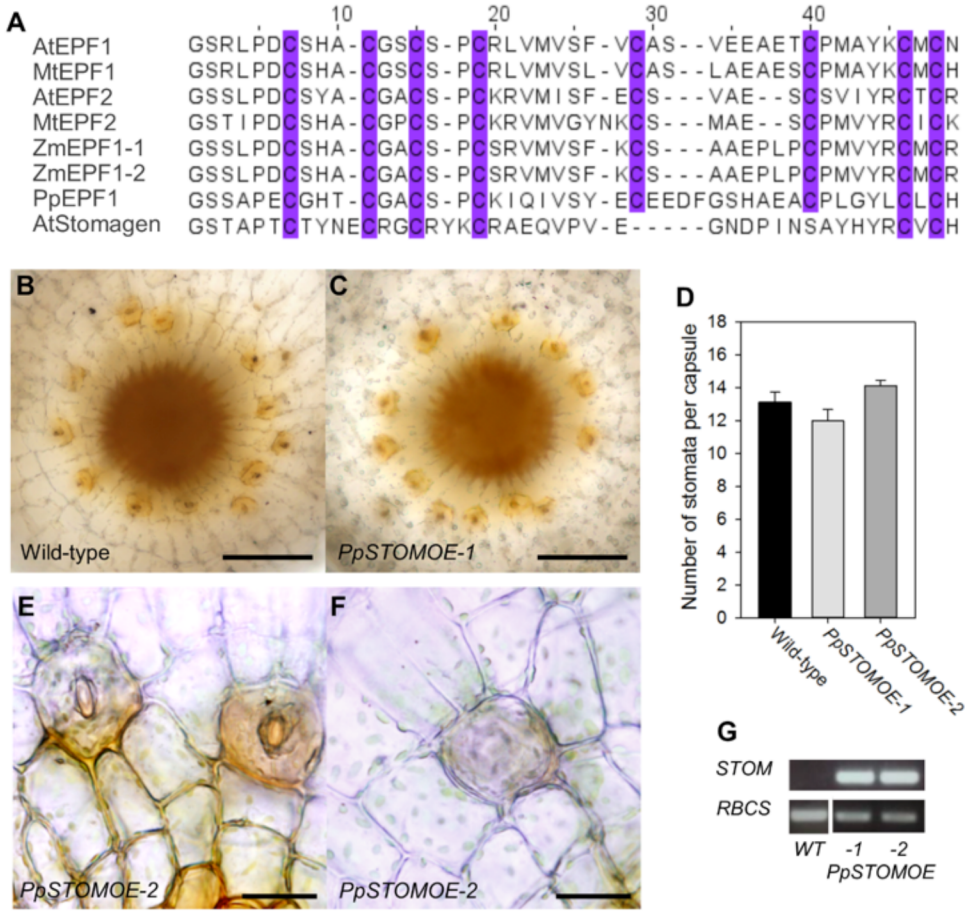

Fig. S4 Overexpression of *STOMAGEN* (*AtEPFL9*) does not disrupt stomatal patterning in *Physcomitrella patens*.

(A) Sequence alignment of EPF peptides. Conserved amino acids are highlighted in purple. (B,C) Bright field images of the base of the sporophyte from (B) WT and (C) PpSTOMOE-1 plants (D) Number of stomata per capsule in wild-type and two PpSTOMOE lines. No significant difference ($P < 0.05$) was found between the lines (oneway ANOVA with multiple comparisons corrected using a Dunnett's test, n=7). (E,F) Images showing abnormal cell division patterns at the base of sporophytes in PpSTOMOE lines. (G) RT-PCR analysis of *STOMAGEN* transcript accumulation (upper panel) in two PpSTOMOE lines and WT tissue, and transcript detection for a control RBCS gene (lower panel).

Scale bars: B,C= 100µm; E,F = 25µm; Error bars in D = s.e.m.

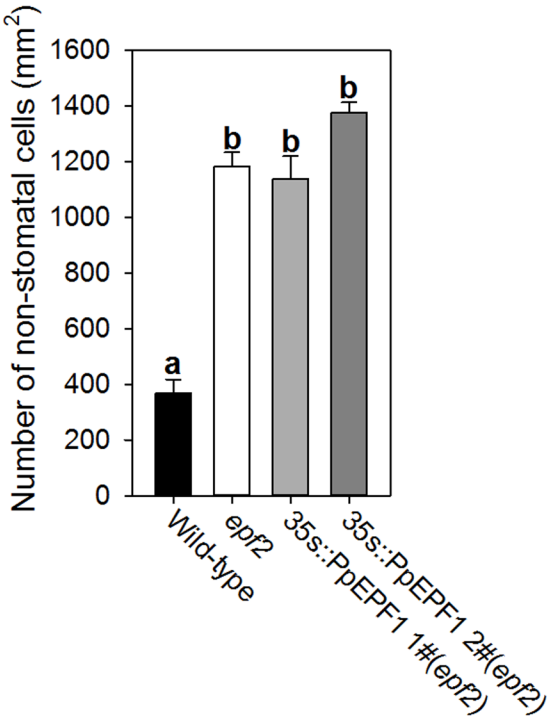

Fig. S5. Expression of *PpEPF1* in the Arabidopsis *epf2* background does not restore WT epidermal cell density. There is a significant increase in epidermal cell density relative to WT in both the *epf2* mutant and in two lines of the *epf2* mutant overexpressing *PpEPF1* (One-Way ANOVA with multiple comparisons corrected with a Dunnett test, n=6, $p < 0.001$ for columns indicated with different letters).

Gene identifier	Accession 1	Accession 2
PpEPF1	Pp3c6 27020V3.1	Pp1s279 24V6.1
PpCHALLAH-related1	Pp3c23_5720V3.1	Pp1s16_10V6.1
PpCHALLAH-related2	Pp3c24_9860V3.1	Pp1s196_93V6.1
PpCHALLAH-related3	Pp3c23_11350V3.1	Pp1s137_142V6.1
PpCHALLAH-related4	Pp3c17_10490V3.1	Pp1s105_161V6.1
PpCHALLAH-related5	Pp3c5_11260V3.1	Pp1s263_75V6.1
PpCHALLAH-related6	Pp3c6 12270V3.1	
PpCHALLAH-related7	Pp3c16_1430V3.1	Pp1s144_136V6.1
PpCHALLAH-related8	Pp3c2_13490V3.1	Pp1s30_64V6.1
PpCHALLAH-related9	Pp3c1 26030V3.1	Pp1s21_79V6.1
ZmEPF1-1	GRMZM2G177393	
ZmEPF1-2	GRMZM2G431783	
MtEPF1	Medtr2g090220.1	
MtEPF2	Medtr2g067510.1	
StEPF1	PGSC0003DMG400007864	
StEPF2	PGSC0003DMG400027541	
AtEPF1	AT2G20875.1	
AtEPF2	AT1G34245.1	
AtEPFL1	AT5G10310.1	
AtEPFL2	AT4G37810.1	
AtEPFL3	AT3G13898.1	
AtEPFL4/CLL2	AT4G14723.1	
AtEPFL5/CLL1	AT3G22820.1	
AtEPFL6/AtCHALLAH	AT2G30370.1	
AtEPFL7	AT1G71866.1	
AtEPFL8	At1g80133.1	
AtEPFL9/AtSTOMAGEN	AT4G12970.1	
AtCLAVATA3	AT2G27250.3	
PpTMM	Pp3c3_3780V3.1	Pp1s1_587V6
SmTMM	125817	
ZmTMM	GRMZM2G011401	
MtTMM	Medtr2g103940.1	
StTMM	PGSC0003DMG400028627	
AtTMM	AT1G80080.1	
AtRLP29	AT2G42800.1	
AtRIC7	AT4G28560.1	
PpERECTA1	Pp3c2_22410V3.1	Pp1s125_96V6.1
PpERECTA2	Pp3c1_17360V3.1	Pp1s63_16V6.1
PpERECTA3	Pp3c21_9500V3.1	Pp1s353_18V6
PpERECTA4	Pp3c18_10870V3.1	Pp1s19_291V6
PpERECTA5	Pp3c22_10630V3.1	Pp1s121_69V6
PpERECTA6	Pp3c19_15110V3.1	Pp1s20_166V6
ZmERECTA1	GRMZM2G463904	
ZmERECTA2	GRMZM5G809695	
ZmERL1	GRMZM2G082855	

MtERECTA	Medtr1g015530.1	
MtERL1	Medtr1g102500.1	
AtERECTA	AT2G26330.1	
AtERL1	AT5G62230.1	
AtERL2	AT5G07180.1	
AtBAM1	AT5G65700.1	
AtBAM2	AT3G49670.1	
AtBAM3	AT4G20270.1	
AtCLAVATA1	AT1G75820.1	

Table S1. Accession numbers relating to gene identifiers used in the phylogenetic analyses.
For *P. patens* both V3.3 and V1.6 identifiers are provided.

Primer name	Sequence
5’ PpEPF1 3’ F	CTCTCACTCCTCAATACACGTG
5’ PpEPF1 3’ R	GCAACAAACGTCATTTCCAA
PpEPF1 KO CONSTRUCT F	AGCGCAATCCACATACGAAACT
PpEPF1 KO CONSTRUCT R	GGGTTGGGCGAAGGTTTTATATT
Flanking PpTMM 5’ F	GTGCATTAACGGTGCATTGAAA
Flanking PpTMM 5' R	GCATCTGACACGAAATGTCACAG
Flanking PpTMM 3’ F	TTCAACCTTCCCAATGCACCTAT
Flanking PpTMM 3’ R	CACTCATACTTTTGGACCGATGC
PpTMM KO CONSTRUCT F	GATGGAGGTGGTCCTACGAGAG
PpTMM KO CONSTRUCT R	GCGGATTGATAAATTGGCGTTA
Flanking PpERECTA1 5’ F	CTCGCTCTCTCTCTTCCTGG
Flanking PpERECTA1 5' R	ATCGCCATGACAGGGAGTAG
Flanking PpERECTA1 3’ F	TCCACTCCACTTCCCATTCT
Flanking PpERECTA1 3’ R	GGTGACTTCCTATCATGCGC
PpERECTA1 KO CONSTRUCT F	CTCGCTCTCTCTCTTCCTGG
PpERECTA1 KO CONSTRUCT R	GGTGACTTCCTATCATGCGC
PpEPF1 OE F	GCCTTATTGACATGGCTGCT
PpEPF1 OE R	TCAAGGGATGGGAAAGGATT
PpTMM OE F	ATTGTGGTAGTGTACGAGGTAGGC
PpTMM OE R	TTAGCACCTTGACATGATTACGA
AtSTOMAGEN OE F	AAGCATGAAATGATGAACATCAAG
AtSTOMAGEN OE R	TTATCTATGACAAACACATCTATAATGAT
M13 F	GTAAAACGACGGCCAGT
M13 R	CAGGAAACAGCTATGAC
PpEPF1 OE CONSTRUCT F	ACCATGAGCAACGAGCTGAA
PpEPF1 OE CONSTRUCT R	AACAGCACATAGGCCGACAA
PpTMM OE CONSTRUCT F	ACCATGAGCAACGAGCTGAA
PpTMM OE CONSTRUCT R	TGCCTCGGTAACATCTTCAGG
AtSTOMAGEN OE CONSTRUCT F	GGTCGATCTGGTTGTACTGAGG
AtSTOMAGEN OE CONSTRUCT R	AACAGCACATAGGCCGACAA
PpEPF1 RT-PCR F	CCGCGTCATACTTGGAACTG
PpEPF1 RT-PCR R	CAAGTAGCCCAACGGACAAG
PpEPF1 OE RT-PCR F	TCCAAGATAGAGACTGAGGGG
PpEPF1 OE RT-PCR R	TCCTCGCATTCATAGCTCACAA
PpTMM RT-PCR F	TGGCGCACAACAGATTCTCAGG
PpTMM RT-PCR R	AGCCTTCGTTGTTCTGCAGTCG
PpTMM OE RT-PCR F	CTCCAACAACCAAAGCGTCG
PpTMM OE RT-PCR R	AACGCTGGTTTTAAGCTGCC
PpERECTA1 RT-PCR F	TAAGCGAGAAGTACGTGGCA
PpERECTA1 RT-PCR R	GGATAACTGGGAGGTTTGCG
PpAtSTOMAGEN OE RT-PCR F	GTTCAAGCCTCAAGACCTCG
PpAtSTOMAGEN OE RT-PCR R	CCTTCGACTGGAACTTGCTC
PpRubisco RT-PCR F	TTGTGGCTCCTGTCTCTGTG
PpRubisco RT-PCR R	CGAGAAGGTCTCGAACTTGG
PpEPF1 comp AtEPF1 F	CACCATGGCCTTATTGACATGG
PpEPF1 comp AtEPF1 R	TCAAGGGATGGGAAAGGAT
pAtTMM F	CACCATACAATCCATGATGCTGCTT
pAtTMM R	CATTTCTTAGTTGTTGTTGTTGTGT
PpTMM comp AtTMM F	CACCATGATTGTGGTAGTGTACG
PpTMM comp AtTMM R	TTAGCACCTTGACATGATTACGAG

qPCR PpERECTA1 F	CTTCGGTATTGTGCTGCTGG
qPCR PpERECTA1 R	CTTCGCACACAACAACGCTA
qPCR Adenine phosphoribosyltransferase F	AGTATAGTCTAGAGTATGGTACCG
qPCR Adenine phosphoribosyltransferase R	TAGCAATTTGATGGCAGCTC
qPCR Small Ribosomal F	ACGGACATTGCATTTAAGACCT
qPCR Small Ribosomal R	GTCGATTACCTGTGGAGAAGAC
qPCR Large Ribosomal F	GACAGGCACAGGGTATTCCT
qPCR Large Ribosomal R	ATCTTCCGTCGTGTTGATCC

Table S2. Primers used in this study